Future changes in wet and dry season characteristics in CMIP5 and CMIP6 simulations

Article

Accepted Version

Future Changes in Wet and Dry Season Characteristics in CMIP5 and CMIP6 simulations

Caroline M. Wainwright*

Department of Meteorology, University of Reading, Reading, UK and National Centre for Atmospheric Science, UK

Emily Black

Department of Meteorology, University of Reading, Reading, UK and National Centre for Atmospheric Science, UK

Richard P. Allan

Department of Meteorology, University of Reading, Reading, UK and National Centre for Earth Observation, Reading, UK

Corresponding author: Caroline M. Wainwright, c.wainwright@reading.ac.uk

ABSTRACT

Climate change will result in more dry days and longer dry spells, however, the resulting impacts on crop growth depend on the timing of these longer dry spells in the annual cycle. Using an ensemble of Coupled Model Intercomparison Project Phase 5 and Phase 6 (CMIP5 and CMIP6) simulations, and a range of emission scenarios, here we examine changes in wet and dry spell characteristics under future climate change across the extended tropics in wet and dry seasons separately. Delays in the wet seasons by up to two weeks are projected by 2070-2099 across South America, Southern Africa, West Africa and the Sahel. An increase in both mean and maximum dry spell length during the dry season is found across Central and South America, Southern Africa and Australia, with a reduction in dry season rainfall also found in these regions. Mean dry season dry spell lengths increase by 5-10 days over north-east South America and south-west Africa. However, changes in dry spell length during the wet season are much smaller across the tropics with limited model consensus. Mean dry season maximum temperature increases are found to be up to 3°C higher than mean wet season maximum temperature increases over South America, Southern Africa and parts of Asia. Longer dry spells, fewer wet days, and higher temperatures during the dry season may lead to increasing dry season aridity, and have detrimental consequences for perennial crops.

1. Introduction

Climate change will result in more dry days and longer dry spells; this has the potential to lead to negative impacts on crop yields and food security, as water stress limits crop growth. Across the tropics most crops are grown solely during the annual wet season, with few crops grown during the dry season. Therefore the timing of these longer dry spells in the annual cycle is of crucial importance in determining their impact.

As the climate warms, the contrasting constraints of energy budgets at global scales and moisture budgets at regional scales drive a general increase in precipitation intensity and decrease in frequency that are further altered as atmospheric circulation patterns shift in location (Trenberth 2011; Held and Soden 2006; Funk et al. 2019; Giorgi et al. 2019; Allan et al. 2020). A larger increase in precipitation intensity compared to mean precipitation is balanced by a decrease in the number of wet days, resulting in longer dry spells and shorter wet spells (Giorgi et al. 2011; Seneviratne et al. 2012; Sillmann et al. 2013b). These longer dry spells may have negative impacts on crop yields and food production (Rockström et al. 2010), as reductions in water availability limit crop growth. Heavier rainfall events punctuating longer dry spells can also affect hydrological characteristics; for example, more rainfall can be taken up by the soil rather than producing runoff yet on the other hand, more intense rainfall falling on encrusted ground can lead to higher runoff (Eekhout et al. 2018; Yin et al. 2018).

Many studies have reported an increase in the number of dry days and dry spell lengths under future climate change. Giorgi et al. (2019) found an increase in the number of dry days and dry spell lengths and a decrease in wet spell lengths aggregated over land areas in the tropics and the extra-tropics over the 21st century in 10 Coupled Model Intercomparison Project Phase 5 (CMIP5) model projections. Giorgi et al. (2014) report that the response in wet and dry spell lengths is more

pronounced and spatially consistent over the tropics than the extratropics. Polade et al. (2014) also identified an increasing dry day frequency, in particular over northern South America, Central America, Southern Africa and the Mediterranean; regions also identified by Pascale et al. (2016) as showing increases in the number of dry days. While Giorgi et al. (2014) and Giorgi et al. (2019) examined the mean wet and dry spell lengths over large land areas, Sillmann et al. (2013b) looked at the maximum wet and dry spell lengths over a number of regions. They find significant increases in maximum dry spell length over Central America, parts of South America, the Mediterranean, Southern Africa, and south and south-east Asia, (consistent with the regions where Polade et al. (2014) found more dry days) with decreases in maximum dry spell length over the high northern latitudes, north-east Asia and East Africa. Lau et al. (2013) also suggest increasing dry spell lengths over Southern Africa, the Mediterranean and parts of South America, although they use a threshold of <0.024 mm day^{-1} to look at the changes in the frequency of dry months. Overall, the Intergovernmental Panel on Climate Change (IPCC) Special Report on Extremes concluded that an increase in dry spell length and frequency was very likely over the Mediterranean and southern Australia, and likely over most subtropical regions (Seneviratne et al. 2012).

Most of these previous studies have looked at changes in wet and dry spells across the entire calendar year (Sillmann et al. 2013b). In the tropics, however, most crops are grown during the annual wet season. Therefore the impact of longer or shorter wet and dry spells may vary throughout the year. Longer dry spells during the main wet season may have significant detrimental impacts on agriculture, whereas longer dry spells within the period of the year that is climatologically dry may have less impact. Conversely, longer wet spells within the dry season may be beneficial e.g. for recharging water supplies. Therefore, understanding the timing of changes in wet and dry spell lengths is of crucial importance. Orlowsky and Seneviratne (2012) looked at changes in consecutive dry days (CDD) in the four meteorological seasons and found some differences in

the projected changes in different seasons; for example, over Asia there is a decrease in CDD in December-February (DJF), but an increase in June-August (JJA). The magnitude of changes was also different in different seasons; for example, over Southern Africa the increase in CDD was greater in JJA than in DJF. However, these 3-month meteorological seasons may not map directly onto wet and dry seasons and there may be changes in wet and dry season length in the future (Dunning et al. 2018). Other studies looking at changes in wet and dry spell lengths in wet seasons have focused over certain regions, for example, Klutse et al. (2018) looked at changing wet and dry spell lengths in June-September over West Africa, and Mba et al. (2018) examined changing wet and dry spell lengths in March-May and September-November over Central Africa. Furthermore, very few studies have also considered the impact of temperature changes; increases in temperature combined with longer dry spells may lead to reductions in soil moisture and increased water stress for crops. Changes in extreme temperatures may differ in wet and dry seasons, hence it is important to separately examine the wet and dry seasons, so as not to exaggerate the impact of temperature changes on agriculture.

Although the seasonal timing of changes in wet and dry spells is of significant societal importance, it has not been investigated consistently in previous studies. Many studies have found a trend of wet seasons getting wetter and dry seasons getting drier under future climate change (Chou et al. 2013; Kumar et al. 2015; Schurer et al. 2020), suggesting there may be notable seasonal differences in wet and dry spell projections. Thus, the aim of the present study is to answer the question "Do changes in the length of wet and dry spells differ in climatologically wet and dry seasons?". Unlike previous dry spell studies, a recently developed methodology is used to determine the timing of the wet and dry season at each location (Liebmann et al. 2012; Dunning et al. 2016), thus enabling investigation of changes in the wet and dry season using a location-specific, not month-based, seasonal definition. Furthermore, we utilise projections from the latest version of

coupled global climate models, which have recently been released (Coupled Model Intercomparison Project Phase 6, CMIP6, Eyring et al. 2016); these are of higher resolution with more complex models than the previous generation of coupled global climate models (CMIP5, Taylor et al. 2012), and thus represent a new opportunity for exploring changes in daily quantities. Here, results from both CMIP5 and CMIP6 are compared, using a range of emissions scenarios. Many previous studies have used the well-established Climdex (`https://www.climdex.org/`) indices to explore changes in wet and dry spells (Zhang et al. 2011; Seneviratne et al. 2012; Sillmann et al. 2013b). These define CDD (Consecutive Dry Days; maximum length of dry spell) and CWD (Consecutive Wet Days; maximum length of wet spell) as "the maximum number of consecutive days with daily precipitation less than/greater than 1mm day^{-1}" (for CDD/CWD respectively). This therefore only looks at the longest wet/dry spell in a year. In this study we aim to look at a more complete set of metrics, including number of wet days and mean length of wet/dry spells, to gain a more complete picture of how wet and dry spells are changing under future climate change. Along with changes in wet and dry spells, changes in maximum temperatures are also considered, as large temperature increases may exacerbate the impacts of long dry spells.

2. Data and Methodology

a. Model Data

Daily precipitation data were used from 31 CMIP5 (Coupled Model Intercomparison Project Phase 5, Taylor et al. 2012) models and 19 CMIP6 (Coupled Model Intercomparison Project Phase 6, Eyring et al. 2016) models under a medium (Representative Concentration Pathway (RCP) 4.5/ Shared Socioeconomic Pathway (SSP) 245) and high (RCP8.5/SSP585) emissions scenario; a full list of models used is included in Tables S1 and S2. SSP585 is the highest emissions scenario and

represents an update to the RCP8.5 emissions scenario (the highest emission scenario for CMIP5); both produce a radiative forcing of 8.5 W m^{-2} in 2100 (Van Vuuren et al. 2011; O'Neill et al. 2016). While some have argued that this pathway is unrealistic, it should be noted that current emissions are in line with the RCP8.5 scenario (Schwalm et al. 2020). The SSP245 scenario represents a medium emissions scenario and updates the RCP4.5 pathway; both produce a radiative forcing of 4.5 W m^{-2} in 2100 (Van Vuuren et al. 2011; O'Neill et al. 2016).

Models were selected based on the availability of daily precipitation data for historical and RCP4.5/RCP8.5 (CMIP5) or SSP245/SSP585 (CMIP6) simulations for periods at the end of the 20th and 21st centuries. For the present day climate, the historical simulation was used over the period 1 January 1985 - 31 December 2014, chosen to be in line with IPCC AR6. For the CMIP5 simulations the historical simulation is only available until 31 December 2005; CMIP5 RCP4.5 simulations were used for 1 January 2006 - 31 December 2014 (taken from the same model) and appended to the historical simulations for 1 January 1985 - 31 December 2005. Recent analysis suggests that CO_2 emissions have been above RCP4.5 levels over the recent period, so this gives a conservative estimate (Schwalm et al. 2020). Projections from RCP4.5 and RCP8.5 do not differ significantly over this 2005-2014 period, therefore the choice of scenario was assumed to have a minimal impact. Furthermore, the primary focus is on the newer CMIP6 models; results from the CMIP5 models are mainly presented for traceability with previous studies. The period 1 January 2070 - 31 December 2099 was used for the end of the 21st century period. Only the first ensemble members were used (r1i1p1/r1i1p1f1) – for two CMIP6 models r1i1p1f2 was used due to r1i1p1f1 being unavailable (see Table S2). Other studies have taken a similar approach. Daily maximum temperature data were also used for the same set of models and time periods, however, they were unavailable for a couple of the models at the time when the analysis was conducted; this is indicated in Table S2.

Data were considered over the region 50°S-50°N. The focus here is on differences in wet and dry seasons so the decision was taken to focus on this tropics and sub-tropics region that has a well defined wet season (equatorward parts of mid-latitudes are also included in 50°S-50°N); high latitude regions tend to have less well-defined wet and dry seasons and thus are not included. All analysis was done on the models at native resolution. For the multi-model median maps the metrics were first computed at the native resolution and were then regridded onto the lowest resolution grid using nearest-neighbouring remapping. For the regional analysis the regions were calculated for each model grid and the model's native resolution grid was used.

b. Observational Data

CHIRPS (Climate Hazards group Infrared Precipitation with Stations) precipitation data were used over 50°S-50°N for 1 January 1985 – 31 December 2014 (to be comparable to historical CMIP6 simulations). CHIRPS precipitation estimates use thermal infrared imagery and gauge data in addition to a monthly precipitation climatology, CHPClim (Climate Hazards Center's Precipitation Climatology) and CFS (Coupled Forecast System) version 2 reanalysis fields to produce rainfall estimates (Funk et al. 2015).

c. Methodology

To calculate metrics, including mean wet and dry spell lengths, for wet and dry seasons separately, each grid point is first classified into one of four seasonality categories (section 1), then season start and end dates are computed using a methodology for objectively calculating wet season onset and cessation dates (section 2). Metrics are then calculated for wet and dry seasons separately (section 3).

1) Seasonality Classification

The seasonality of precipitation varies across the tropics from monsoonal regions with one summer wet season per year, to dry desert regions with little rainfall, to rainforest regions that are wet year round. East Africa is known to experience two wet seasons per year (Yang et al. 2015). To distinguish between wet and dry seasons, it is first important to determine the seasonal regime.

A number of different methodologies have been utilised for this purpose; Herrmann and Mohr (2011) used monthly precipitation and temperature to define rainfall seasonality regimes across Africa. Pascale et al. (2016) and Feng et al. (2013) used the Relative Entropy and Dimensionless Seasonality Index to define and examine changes in the 'Global Monsoon Domain'. Liebmann et al. (2012) and Dunning et al. (2016) use harmonic analysis to separate regions with one or two wet seasons per year across Africa. A combination of these metrics is used here.

It was decided that four categories need to be distinguished: regions that are dry year-round, regions that are wet year-round, regions with one wet season per year (annual regime), and regions with two wet seasons per year (biannual regime). While Herrmann and Mohr (2011) defined additional regimes, here just four are used for simplicity. The methodology used has three steps:

1. The mean annual rainfall was computed at each land grid point (between 50°S and 50°N). The 20% of driest land grid points were excluded as dry regions with no marked wet season.

2. Grid points with a relative entropy (a measure of how uniform or variable the seasonal sequence of monthly rainfall is, see below) less than 0.3 were defined as wet year round with no marked wet/dry seasons.

3. The remaining grid points were defined as having one/two wet seasons per year based on the ratio of the amplitude of the second harmonic to the amplitude of the first harmonic. If the

ratio is greater than 1/less than 1 then the grid point experiences a biannual/annual regime with two/one wet season(s) per year.

The relative entropy quantifies how different the observed sequence of monthly rainfall is from a uniform monthly sequence with unchanging monthly rainfall. The relative entropy attains the maximum value when the annual rainfall is concentrated in one single month, and equal to 0 for a uniform precipitation sequence (Feng et al. 2013; Pascale et al. 2016). Details of the calculation of relative entropy are in the Supplementary Information.

Regions that are wet year round have a low value of relative entropy. Pascale et al. (2016) defined the 'Global Monsoon Domain' to be where $D_k > 0.4$ (and where the Dimensionless Seasonality Index is >0.05, but this is mainly used to remove dry regions), but when examining changes in the timing of the rainfall centroid Pascale et al. (2016) used a relative entropy threshold of 0.3 to "exclude regions without a pronounced dry season". Here a threshold of 0.3 is used; a range of thresholds were considered and it was decided that a D_k threshold of 0.3 classified regions such as the Maritime Continent, Central Africa and eastern North America, known to be wet year round, correctly, while also classifying most of South America as having an annual regime. The aim was to just exclude those points that are definitely wet year round (without a pronounced dry season), as opposed to just including those with a well-defined monsoon, hence the threshold of 0.3 was used.

The seasonality classification for CHIRPS (Figure 1) shows that the dry desert regions (including the Sahara and Gobi Deserts, and the Arabian Peninsula) are correctly identified as dry-year-round, Central Equatorial Africa and the Maritime Continent are correctly identified as wet year-round, and the Horn of Africa is categorised as biannual. Monsoon regions, such as India, East Asia and South America are correctly identified as experiencing an annual regime. Over Africa, the

classification is similar to that produced by Herrmann and Mohr (2011). This classification gives an overall picture – in regions of complex rainfall regimes, with multiple rainfall peaks separated by a relatively drier period lasting only one to two months (e.g. Central America; Small et al. 2007) it may not capture this complex seasonal regime, and defines the region as having one wet season per year.

The seasonality classification was calculated for each model and scenario; it was calculated separately for the present and future periods. Figure 1 shows the seasonality mask for CHIRPS, and the modal seasonality classification for CMIP6 historical (for CMIP5 and all scenarios see Figure S1). For the most part the model seasonality classification shows good agreement with CHIRPS with a few minor differences; southern Australia and eastern China are shown as having one wet season in models whereas they are defined as wet year round in observations. In terms of the future projections there are not large changes in the overall pattern of seasonality (<10% of grid points change regime), and most changes are located on regime boundaries (Figure S1). The notable changes are over southern Europe/middle East where we see changes from wet year round to an annual regime, and over central Africa CMIP6 shows some grid points change from wet year round to two wet seasons per year; presumably due to larger rainfall increases in the wetter seasons than the drier seasons.

2) Wet and Dry Season Distinction

The method of anomalous accumulation was used to determine start and end dates of the climatological wet and dry seasons. This method is suitable for application at a global scale as it does not use a set precipitation threshold, and therefore can be applied to regions with very different rainfall amounts (Liebmann et al. 2012; Dunning et al. 2016). It is applicable to regions

with both one and two wet seasons per year (Dunning et al. 2016). Full details of the calculation can be found in the Supplementary Information.

Onset and cessation dates were calculated for each model and scenario; thus accounting for changing seasonal timing under future climate change. Historical patterns of onset and cessation in the CMIP5 and CMIP6 models were similar to those produced using observations, with a wet season during the boreal summer in the northern hemisphere and a wet season during the austral summer in the southern hemisphere (see Figure S2-6 in the Supplementary Information); Dunning et al. (2017) showed that CMIP5 models generally captured the correct patterns of onset and cessation across Africa, when assessed using this methodology.

3) Wet and Dry Spell Metrics

A range of metrics were calculated for wet and dry seasons. The wet season was defined to be the period after the onset and before the cessation date, while the dry season was defined to be the period between the cessation date and the onset date. For the metrics calculated here, a threshold of 1 mm day^{-1} was used to define a wet/dry day. The well-established Climdex indices also use a threshold of 1 mm day^{-1} to define wet/dry days for the calculation of CWD and CDD, used in Seneviratne et al. (2012) and Sillmann et al. (2013b). Other studies looking at wet and dry days and spells also use a threshold of 1 mm day^{-1} (Polade et al. 2014; Giorgi et al. 2014; Funk et al. 2019; Giorgi et al. 2019), and this is confirmed by analysis of cumulative frequency of daily rainfall (Figure S7).

The following metrics were calculated:

- Wet/Dry Season Rainfall: Sum of daily rainfall over the wet/dry season.
- Wet/Dry Season Rainy Days: The number of days with rainfall greater than 1 mm day^{-1} in the wet/dry season.

- Wet/Dry Season Rain per Rainy Day: The mean rainfall over all days with rainfall greater than 1 mm day^{-1} in the wet/dry season.

- Maximum wet/dry spell length in wet/dry seasons: The length (in days) of the longest wet/dry spell in each wet/dry season.

- Mean wet/dry spell length in wet/dry seasons: The mean length (in days) of all wet/dry spells (of length two days or more) in the wet/dry season.

- Wet/Dry Season Mean Maximum Temperature: The mean of the daily maximum temperature over the wet/dry season.

Metrics were computed for one wet season for the annual regime region and for two wet seasons for the biannual regime regions. For the wet-year-round regions the metrics were calculated for each calendar year (wet season was assumed to last all year); these points have a wet season but no dry season, so are included in wet season plots but not dry season plots. The median was taken over all seasons and the historical and future periods compared. For the maps, the change was regridded onto the lowest resolution model using nearest-neighbour remapping.

Figure 2 and Figure S8 show that the historical simulations from the CMIP5 and CMIP6 models capture the observed distribution of wet and dry spells in wet and dry seasons as found in CHIRPS. The main difference is the mean length of wet spells in the wet season where the CMIP6 models contain much longer wet spells than the observations. Similarly, Sillmann et al. (2013a) found good model representation of CDD in the CMIP5 models, but found that CWD was overestimated in both models and reanalyses. Results from a second observational dataset (Multi-Source Weighted-Ensemble Precipitation (MSWEP, Beck et al. 2019); Figure S9) are very similar to those shown in Figure 2 for CHIRPS. The mean length of wet spells in the wet season is longer in MSWEP over parts of South America, Ethiopia and the Himalayas in MSWEP, presumably due to the inclusion

of reanalysis data, but the mean lengths in CMIP6 still exhibit a positive bias over these regions when compared with MSWEP.

4) Regions

To explore changes over certain regions a regional classification was required. The regions used here are those defined for the 6th IPCC report (Iturbide et al. 2020). The locations and regions used are shown in Figures 6a, 8a and 10a.

5) Timeseries Analysis

Timeseries were produced for certain regions to examine the changes over the whole period (1985-2099). The regions for timeseries were selected over areas of particular interest, where significant changes in wet/dry spell length had been identified. For the timeseries it is assumed that all grid points have an annual regime; for the three regions used (NES, SEAF and WAF) this is a reasonable assumption (Figure 1).

When calculating the timeseries of wet/dry spell lengths over the IPCC regions two methodologies were employed. The first methodology defined a climatological onset and cessation date using the full 115 years of the timeseries and then used the same onset and cessation date for each year, thus not accounting for changes in seasonal timing. The wet and dry spell lengths were then calculated for each year, in the same manner as above. The second methodology used a moving 30-year period to calculate the onset and cessation dates, with the first 15 and last 15 years of the full record set to the first-30-years value and the last-30-years value. Thus this second methodology takes into account changes in seasonal timing. In section 3, timeseries produced using the second methodology were presented. For the most part the differences between the two methodologies were similar.

3. Results and Discussion

Results are presented here for wet and dry seasons; section 3a on seasonal timing presents changes in timing of the onset and cessation of the wet season, while sections 3b-3e present changes in rainfall and temperature metrics for wet and dry seasons separately. Figure S2 in the Supplementary Information indicates the timing of the wet season(s) in the calendar year for reference.

a. Seasonal Timing

The multi-model median change in onset and cessation of the annual wet season in CMIP6 under the SSP585 scenario, shown in Figure 3, shows that onset is projected to get later across South America, Southern Africa, West Africa and the Sahel, with changes of up to two weeks. Over South America this continues the recent trend of delayed onset found by Correa et al. (2020). Over East Asia Figure 3 shows the onset is projected to be earlier, with advances of over a week in some locations. Changes in cessation are smaller than changes in onset; Figure 3b shows later cessation by up to a week over the Sahel, and parts of Asia, with the largest changes of around two weeks over central America. These results show good agreement with previous studies of changing onset over Africa (Dunning et al. 2018), and over Asia, with Kitoh et al. (2013) reporting a later retreat over South Asia and Ha et al. (2020) reporting an earlier onset over East Asia. The results also show good agreement with Pascale et al. (2016), who analysed changes in the timing of the rainfall centroid, and found a delay over Africa, Central and South America and parts of South Asia, with an advance over East Asia. More broadly, a number of studies have found a global phase delay of the seasonal cycle of precipitation (Biasutti and Sobel 2009; Dwyer et al. 2014; Marvel et al. 2017) and a redistribution of rainfall from early to late in the monsoon season (Seth et al. 2013), in agreement with the generally later onset/cessation shown in Figure 3. A number of mechanisms have been proposed for this; Dwyer et al. (2014) linked the delay to changes in the seasonality of

the circulation, Seth et al. (2013) linked the delay to an enhanced spring convective barrier, while Song et al. (2018) linked the delay to changes in cross-equatorial energy transports and change in the strength of the subtropical highs.

b. Seasonal Rainfall Characteristics

Firstly, changes in seasonal rainfall totals, seasonal number of rainy days and seasonal rain per rainy day were explored; Figure 4 shows the changes from CMIP6 under SSP585. South and East Asia, Eastern Africa and Eastern North America all show projected increases in wet season rainfall (Figure 4a); due to a combination of increasing rainfall intensity in the wet season (Figure 4e) and either limited change or a slight increase in the number of wet days in the wet season (Figure 4c). Wang et al. (2021), Wang et al. (2020) and Collins et al. (2013) also show an increase in boreal summer rainfall over South and East Asia; Wang et al. (2020) show increases of around 1 mm day^{-1} in JJAS over South and East Asia. The Mediterranean, Central America and northern South America exhibit significant decreases in wet season rainfall (of 5-25%, Figure 4a); these regions also experience a significant decrease in the number of rainy days in the wet season (decrease of over 15 days, Figure 4c), and smaller increases in rain per rainy day (Figure 4e). The asymmetry between the American and Asian-African monsoon systems, with the North American monsoon getting drier and the Asian-African monsoon getting wetter, identified in other studies (e.g. He et al. 2020), is apparent in Figure 4. Other regions, including Southern Africa, the Maritime Continent, and parts of southern Europe, also exhibit a decrease in the number of wet season rainy days (Figure 4c). However, a significant decrease in rainfall is not found in these regions (Figure 4a) as the decrease in the number of rainy days is compensated by an increase in rain per rainy day (Figure 4e), broadly consistent with expectations from joint thermodynamic and energetic constraints (Allen and Ingram 2002; Trenberth 2011).

Considering the dry season, Central America, South America, Southern Africa and Australia all show decreases in dry season rainfall (Figure 4b), decreases in the number of wet days in the dry season (Figure 4d) and little change in dry season rain per rainy day (Figure 4f). A decrease in boreal summer rainfall over Southern Africa is also found by Wang et al. (2021), Wang et al. (2020), and Collins et al. (2013), and a number of studies have identified an increasing contrast between wet and dry seasons, with wet seasons getting wetter and dry seasons getting drier (Chou et al. 2013; Kumar et al. 2015; Polson and Hegerl 2017; Lan et al. 2019; Deng et al. 2020; Schurer et al. 2020). Eastern Africa, the Eastern Sahel and East Asia all show increases in dry season rainfall (Figure 4b), increases in the number of dry season rainy days (Figure 4d) and increases in dry season rain per rainy day (Figure 4f). Rainfall increases over East Asia are in good agreement with Wang et al. (2021), Wang et al. (2020), and Collins et al. (2013) who identified increased boreal winter rainfall in this region. In general, the increases in dry season rain per rainy day are less than the increases in wet season rain per rainy day. Changes in seasonal rainfall are shown as a percentage of the wet/dry season rainfall; thus while changes in dry season rainfall may appear larger, in absolute terms the changes in wet season rainfall are larger. Central and northern South America show rainfall decreases in both seasons, in agreement with Wang et al. (2020) who also show precipitation decreases over the region in boreal summer and winter, although in winter they find increases over the east and west coast, although it should be noted that they use a month-based seasonal definition, and the increases are very close to the coast, which may have been removed in the land-sea mask applied here.

Changes from CMIP6 under SSP245 and from CMIP5 under RCP8.5 (Figure S10-11) were generally of the same sign of those shown in Figure 4, but of lower magnitude, possibly related to the higher climate sensitivity in CMIP6 than in CMIP5 (Meehl et al. 2020). Over northern South America decreases in dry season rainfall were ubiquitous, but decreases in wet season rainfall were

only found in CMIP6 under SSP585. Although they all show a decrease in the number of wet season rainy days over northern South America, CMIP5 RCP8.5 shows a larger increase in wet season rain per rainy day, and CMIP6 SSP245 has a smaller decrease in the number of rainy days, but similar change in rain per rainy day to CMIP6 SSP585. Increases in wet season rainfall over Eastern Africa and South and East Asia, and increases in dry season rainfall over East Africa and East Asia, were found to be robust across the three scenarios and CMIP eras. Decreases in dry season rainfall over Southern Africa were present in all three scenarios and CMIP eras, but were only significant under SSP585 and RCP8.5.

c. Wet and Dry Spells

Figure 5 shows the projected changes in the mean length of wet and dry spells in wet and dry seasons from CMIP6 under SSP585; the changes in maximum spell length are generally of the same sign and of larger magnitude (see Figure S14).

During the dry seasons, projections indicate longer dry spells over Central America, north-east South America, Southern Africa and Australia, with increases of up to 10 days (Figure 5a). This is consistent with Figure 4 which showed reductions in dry season rainfall and fewer dry season rainy days over these regions. Shorter dry spells in the dry season are found over East Africa and parts of the Sahel, and East Asia (Figure 5a); these regions showed increases in dry season rainfall and more rainy days in the dry season (Figure 4). Orlowsky and Seneviratne (2012) also show increases in CDD over Southern Africa in JJA (local dry season). Over northern South America, Orlowsky and Seneviratne (2012) show increases in CDD in different regions in all four seasons, with the smallest increases in DJF (the peak of the wet season), thus agreeing on the projection of longer dry spells in the dry season, but also demonstrating the impact of different definitions

of seasonality. Sillmann et al. (2013b) also show large increases in CDD over north-east South America, Southern Africa, Australia and central America.

For the mean length of dry spells in the wet season (Figure 5b) the changes are generally very small (multi-model median is generally less than half a day) and not statistically significant. Only Southern Europe and the northern Mediterranean shows a statistically significant increase in dry spell length in the wet season; the signal is also seen over the same region for dry seasons (Figure 5a). Parts of the Mediterranean are classified as having one wet season per year, while other parts are wet year round, thus Figure 5a-b indicates a general increase in dry spell length in this region. Other studies, including Orlowsky and Seneviratne (2012) and Seneviratne et al. (2012) show increases in CDD in the Mediterranean; and Brogli et al. (2019) show year-round decreases in Mediterranean rainfall.

The changes in the mean length of wet spells are generally of smaller magnitude than the changes in the mean length of dry spells (Figure 5c-d). The only statistically significant change in the mean length of wet spells in the dry season is over northern South America, which shows a decrease in the mean length of wet spells in the dry season; but the magnitude of the change is small (Figure 5c). Only two regions show significant changes in the mean length of wet spells in the wet season (Figure 5d); Central and northern South America and West/Central Africa both show decreases of less than five days. These are the regions with the longest wet spells during the wet season in current climate (Figure 2), and therefore are likely to exhibit the largest changes. These regions also show fewer wet season rainy days under future climate change (Figure 4c), consistent with shorter wet spells.

Again, changes from CMIP6 under SSP245 and from CMIP5 under RCP8.5 (Figure S12-13,S15-16) were generally of the same sign of those shown in Figure 5, but of lower magnitude. For the mean length of dry spells in the dry season, increases were present across Central America, north-

east South America, Southern Africa and Australia in all three scenarios and CMIP eras, but the magnitude and statistical significance was reduced, particularly under SSP245 where only Southern Africa and small parts of South America showed a statistically significant increase. For the mean length of wet spells in the wet season, the signal was similar in CMIP5 RCP8.5 to CMIP6 SSP585, but much reduced in CMIP6 SSP245, with only the decrease over northern South America present.

Figure 3 showed changes in the length of wet and dry seasons under future climate change, which may affect the length of wet and dry spells. Therefore the analysis was repeated, calculating wet and dry spell lengths as a percentage of the wet/dry season length; results were similar demonstrating that the changes found here are not a consequence of changing season lengths.

Overall, Figure 5a-b indicates that the significant increases in dry spell length expected under future climate change are projected to occur during the dry season not the wet season. Only parts of the Mediterranean and southern Europe, where some locations experience rainfall year round, show a significant increase in dry spell length in the wet season. Therefore agriculture grown solely during the wet season may be less affected by longer dry spells. However, Figures 4-5 indicate longer dry spells, fewer rainy days, and less rainfall during the dry season in certain regions, which may make the dry seasons more intense, negatively impacting perennial crops and crops grown during the dry season.

d. Regional Changes

Figures 4-5 have presented changes across the tropics; three regions are now considered in more detail. Some of the largest changes in wet and dry spell lengths identified in Figures 4-5 were for northern South America and Africa; hence these regions are explored further. South and East Asia is a region of high population density, highly dependent on agriculture, so this region has also been considered in more detail.

1) Northern South America

Decreases in precipitation over northern South America under future climate change have been widely reported (Scheff and Frierson 2012; Wang et al. 2020), and linked to changes in the tropical Pacific (Parsons 2020) and the response of vegetation to elevated CO_2 (Richardson et al. 2018). Recent declines in dry season precipitation over tropical South America can be attributed to elevated greenhouse gases and land use change (Barkhordarian et al. 2018), while recent increased frequency of dry days over the southern Amazon has been linked to tropical North Atlantic warming and enhanced subsidence of the southern branch of the Hadley cell (Espinoza et al. 2019). Three of the IPCC AR6 regions are considered; South American Monsoon (SAM), north South America (NSA) and north-east South America (NES). Figure 6b-c shows there is generally good model agreement in the projection of longer dry spells in the dry season across all three regions; for all scenarios the 25th percentile (across the models) is above 0. Under the high emissions scenarios for CMIP5 and CMIP6 the median increase in the maximum length of dry spells in the dry season ranges between 9 and 26 days, with median increases in the mean length of dry spells in the dry season between 1.4 and 9.4 days. In their analysis of changes in CWD and CDD over Brazil in the CMIP5 models, Avila-Diaz et al. (2020) also found longer dry spells under future climate change, with the largest increases in the north-east. This is a continuation of the recent trend of longer dry spells in north-east Brazil over 1980-2016 (Avila-Diaz et al. 2020).

For the mean and maximum length of wet spells in the wet season the 25th percentile is below 0 for all regions and scenarios indicating strong model agreement on shorter wet spells in the wet season under future climate change (Figure 6d-e). Under the high emissions scenarios for CMIP5 and CMIP6 median decreases in the maximum length of wet spells in the wet season range between 3 and 13 days, while median decreases in the mean length of wet spells in the wet season range

between 0.6 and 3.7 days. It is interesting to note that the largest changes in dry spell lengths are over NES, while the largest changes in wet spell lengths are over NSA; this is consistent with Avila-Diaz et al. (2020) who found the largest decreases in CWD over the central northern part of Brazil.

For both variables and all the regions the changes are larger for the CMIP6 high emissions scenario than the CMIP5 high emissions scenario; this was also noted in the previous section and is thought to be related to the higher climate sensitivity in CMIP6 than in CMIP5 (Meehl et al. 2020).

Timeseries of mean length of dry spells in the dry season and mean length of wet spells in the wet season for the NES region (Figure 7) show the same patterns of longer dry spells in the dry season and shorter wet spells in the wet season. The dots at the top of each panel indicate when the range of values in that year is statistically significantly different from the range over 1985-2014 and indicates the emergence of the signal from the noise. This suggests that the increase in the mean length of dry spells in the dry season becomes statistically significantly different between 2020 and 2040 (depending on the emissions scenario) whereas the decrease in the mean length of wet spells in the wet season is not statistically significant until 2060-2080 (timings are similar for maximum spell lengths). These times of emergence are indicative, but may not be fully quantified, as we have only used one ensemble member per model. For more robust times of emergence the internal variability should be calculated using a large ensemble. For wet spells in the wet season the change is less significant under the SSP245 scenario and diverges from the SSP585 scenario in the 2060s (Figure 7b). The apparent jump in dry spell length around 2065 is not a model artefact, but reflects the combination of internal variability and the levelling off of warming in the SSP245 scenario. Figure 7 also shows the large interannual variability in these metrics and the large model spread. Two methodologies were used for calculating the timeseries; one using varying season

start and end dates and one using fixed seasons start and end dates (see methodology section 5). The results shown in Figure 7 were the same for both methodologies, indicating the result is robust and insensitive to changing season length. However, for the mean length of dry spells in the wet season and mean length of wet spells in the dry season the signal (increase/decrease respectively) becomes weaker and less statistically significant when varying onset is used (not shown). This indicates that erroneously including parts of the other season when the time-invariant dates are used can influence the calculation of these metrics, and indicates changes occurring in the margins between the seasons.

2) Africa

Projected changes in the mean length of wet and dry spells are not consistent across the African continent (Figure 8, Figure S17). While south-west Africa (SWAF) and south-east Africa (SEAF) show longer dry spells in the dry season (increase in mean and maximum length), with median increases in the maximum length greater than 20 days over SWAF, north-east Africa (NEAF) shows shorter dry spells (median change in the maximum length of dry spells is a decrease of 12 days under CMIP6 SSP585, Figure 8b-c). There is good model agreement in shorter dry season dry spells over NEAF, with the 25th percentile below 0 for all scenarios. Pinto et al. (2016) also found increases in CDD over Southern Africa, with increases of greater than 25 days over Zimbabwe and Botswana, with larger increases under RCP8.5 than under RCP4.5, in agreement with Orlowsky and Seneviratne (2012) and Sillmann et al. (2013b). Over East Africa previous studies report both increases and decreases in dry spell lengths. Over southern Ethiopia, Tegegne et al. (2020) found a decrease in CDD during the 2080s under RCP8.5, in agreement with the findings in Sillmann et al. (2013b). However, Gudoshava et al. (2020) show only small changes (generally less than one day) in CDD in March-May, June-September and October-December over the Horn of Africa; Ogega

et al. (2020) also found no large changes in CDD over Kenya and Uganda. Conversely, Osima et al. (2018) find increasing CDD over the Horn of Africa. Our results here are consistent with the studies of Sillmann et al. (2013b), Orlowsky and Seneviratne (2012) and Tegegne et al. (2020); further detailed studies on this region should explore the range of projections from different studies, taking into account the large variability in model projections over East Africa (Rowell et al. 2015). West Africa (WAF) and Central Africa (CAF) show shorter dry spells in the future (Figure S17), although the changes are smaller than those over NEAF and model agreement is weaker; Sillmann et al. (2013b) show that changes in CDD are not significant over these regions.

Only two regions show notable changes in the length of wet spells in the wet season; WAF and CAF show median decreases of 3-6 days in the maximum length of wet spells (under high emissions scenarios, Figure 8d-e). Changes in the mean length also show decreases. While there is generally good model agreement on shorter wet spells in the wet season over WAF and CAF (for the most part the 25th percentile is below 0), there is a large range across the models, particularly under CMIP5 and over CAF. This may be related to poor model representation of the mean climate over this region in CMIP5 models (Creese and Washington 2018) and to the inclusion of a wet-year-round region in equatorial Africa. Klutse et al. (2018) also found a reduction in CWD in June-September over West Africa, with reductions of up to four days over Nigeria and Guinea under 2°C of global warming. Over central Africa Mba et al. (2018) found decreases in CWD in both March-May and September-November.

Figure 9b shows that the decrease in the length of wet spells in the wet season over WAF becomes statistically significantly different from 1985-2014 at around 2050 under SSP585. However, under SSP245 the change does not become consistently statistically significantly different in the period of this timeseries (up to 2100). For dry spells in the dry season over SEAF the increase in length becomes statistically significantly different from 1985-2014 around 2040-2060, later than was

found for NES (Figure 9a). For dry spells in the dry season the scenarios diverge in the 2060s, while for wet spells in the wet season the scenarios diverge in the 2040s.

3) Asia

Generally, changes in the length of wet and dry spells are smaller and less significant, or exhibit limited model consensus, over Asia. Figure 5 showed significant decreases in the mean length of dry spells in the dry season over north-east China (also found by Han et al. 2018; Dong et al. 2020), but no other significant changes over this region. Figure 10b-c confirms that changes in the length of dry spells in the dry season are generally small. The largest change is an increase of four days in the maximum length of dry season dry spells over South Asia (SAS) under CMIP5 RCP8.5; this change is larger in CMIP5 than in CMIP6 (median in CMIP6 SSP585 is an increase of one day), consistent with the slight increase in dry season rainfall over India found in CMIP6 SSP585, but little change in dry season rainfall found in CMIP5 RCP8.5. While there is an increase in the maximum length of dry spells, the change in the mean length of dry spells is small (less than 0.6 days), indicating that for the most part dry season dry spells are not getting longer. An increase in the maximum, but not the mean also suggests an increase in the variability. This highlights the importance of considering the mean as well as the maximum spell length. There is limited model agreement in these changes. Han et al. (2018) also found little change in CDD over South Asia and South East Asia in their analysis of CMIP5 models. Aadhar and Mishra (2020) concluded that projections based on CMIP6 multi-model ensembles are not reliable over South Asia as projections are different when the whole ensemble is used compared with just those models that correctly represent current climate. Further work is required to investigate this region in more detail.

Figure 10b-c also shows a slight increase in the maximum length of dry season dry spells over south-east Asia (SEA). It should be noted that much of this region experiences a wet-year-round rainfall regime, therefore only a small region (over Myanmar and Thailand) will be contributing to this signal; this is supported by the findings of Ge et al. (2019), who show the largest increases in CDD in the SEA region are over the Myanmar/Thailand peninsula. Figure 10b-c shows the median changes are small (two and three days), and again, only seen in the maximum not the mean, with limited model agreement.

Figure 10d-e shows changes in the length of wet spells in the wet season, with median decreases in the maximum length of two and four days over SEA and little change in other regions. This is consistent with a decrease in the number of wet season rainy days over this region. Again, the change in the mean is small (less than 0.4 days), indicating only the longest wet spells are getting shorter, not all wet spells, and also indicating a change in the variability. While Ge et al. (2019) show increases in CWD in the CORDEX models over SEA, they also find that the increase is larger under 1.5°C of global warming than under 2°C of global warming, and under 2°C of global warming some regions show decreases (e.g. Borneo). 2°C of global warming is reached at around 2040 under SSP585 (O'Neill et al. 2016); therefore if the increased warming continues to decrease the change in CWD, this is consistent with our finding of shorter wet spells. Over East Asia (EAS) the changes are small, consistent with the results in Figure 5.

e. Seasonal Maximum Temperature

Interpreting agricultural implications of precipitation changes cannot be considered in isolation from temperature, as the aridity or dryness over a region is determined by the difference between supply (precipitation) and demand (measured by potential evapotranspiration (PET)) (Dai et al. 2018). Elevated greenhouse gas levels lead to increasing temperatures, which combined with small

changes in relative humidity, lead to large increases in the vapor pressure deficit and widespread increases in PET (Dai et al. 2018). Zhao and Dai (2015) found that rising temperatures and vapor deficits explain most of the projected ubiquitous global PET increase. On the other hand, elevated CO_2 concentrations modify how vegetation responds to changing water availability through a complex and uncertain combination of increased plant growth and increased water use efficiency (Mankin et al. 2019; Peters et al. 2018; Kooperman et al. 2018). Furthermore, rainfall changes exert a substantial influence on temperature changes since less cloud and rainfall increases absorbed solar radiation while drier soils increase the sensible heat fraction. Therefore temperature responses in wet and dry seasons are not expected to be uniform and are thus of considerable additional interest.

Figure 11 shows increasing temperatures across the tropics in both wet and dry seasons, as projected under future climate change. Over northern South America, Southern Africa, and parts of Asia, the increase in dry season maximum temperature is up to 3°C greater than the increase in wet season maximum temperature (Figure 11a-b); Zhou et al. (2015) also found the largest temperature increases over drier regions. In both northern South America and Southern Africa this increase in dry season maximum temperature is combined with a decrease in dry season rainfall (Figure 4b), which may lead to a substantial drying of soils during the dry season, affecting perennial crops. Dai et al. (2018) found large increases in PET and decreases in soil moisture over northern South America and southern Africa. Decreases in soil moisture across northern South America and southern Africa were also reported by Collins et al. (2013) and Zhao and Dai (2015). Furthermore, Zhao and Dai (2015) found decreases in soil moisture (hence increased surface drying) in regions projected to receive higher precipitation amounts, due to fewer wet days and longer dry spells and high temperatures, highlighting the importance of changes in frequency in precipitation, in addition to changes in amount.

The contours on Figure 11 indicate that under the historical simulation over 1985-2014 only northern Australia and the Sahel have mean seasonal maximum temperatures greater than 35°C (dashed contour), whereas by the end of the 21st century under SSP585 parts of India, the Sahel, northern South America and parts of northern Australia may all experience mean dry season maximum temperatures of greater than 35°C (solid contour). This may have negative impacts on crops including sorghum (FAO 2020). However, during the wet season temperatures are generally less than 35°C, except over northern Australia and parts of the Sahel. This may mean that crops grown during the wet season are less impacted by these elevated temperatures.

4. Conclusions

Changes in the mean and maximum lengths of wet and dry spells (and mean maximum temperature) have been calculated separately for the climatological wet and dry seasons using an ensemble of CMIP5 and CMIP6 models across the global tropics and subtropics. An objective methodology is used to classify the seasonality at each location and to determine the timing of the climatological wet and dry season(s); metrics including total seasonal rainfall, number of rainy days, rain per rainy day and the mean and maximum length of wet and dry spells are then calculated for the wet and dry seasons separately.

Our main results are (also summarised in Figure 12):

- Onset of the annual wet season is projected to get later across South America, Southern Africa, West Africa and the Sahel, with changes of up to two weeks. Over East Asia the onset is projected to be earlier. Cessation of the annual wet season is projected to be later over the Sahel, parts of Asia, and central America. These changes are consistent with the projected global phase delay of the seasonal cycle of precipitation under future climate change (Dwyer et al. 2014; Song et al. 2018).

- Changes in the mean and maximum length of dry spells are largest during the dry season. Increasing dry season dry spell lengths were found over central America, north-east South America, Southern Africa and Australia. Shorter dry spells in the dry season are found over East Africa and parts of the Sahel, and East Asia. Changes in the length of dry spells in the wet season are generally small, with only the Mediterranean and southern Europe showing significant increases.

- Statistically significant decreases in the length of wet spells in the wet season are found over Central and northern South America and West/Central Africa.

- For the most part, changes were of the same sign in CMIP5 and CMIP6, but of larger magnitude under CMIP6, possibly related to the higher climatic sensitivity (Meehl et al. 2020).

- The time at which the change becomes statistically significantly different from the historical period varies with metric and region; while the increase in length of dry spells in the dry season over north-east South America is statistically significant around 2020-2040, the decrease in the length of wet spells in the wet season over West Africa is not statistically significant until around 2050. Times of emergence here are indicative; more robust times of emergence could be calculated using a larger ensemble.

- Mean maximum temperature increases are greater for the dry season than for the wet season, with mean maximum dry season temperatures increasing by up to 7°C, particularly over South America, Southern Africa and parts of Asia. While only northern Australia is projected to have large areas with mean maximum wet season temperatures >35°C at the end of the 21st century under SSP585, northern South America, the Sahel, and India are projected to have mean maximum dry season temperatures >35°C at the end of the 21st century under SSP585.

This paper aimed to address the question "Do changes in the length of wet and dry spells differ in climatologically wet and dry seasons?". Here it has been decisively shown, considering both the mean and maximum wet/dry spell lengths (thus considering all wet/dry spells, not just the longest) that changes in the length of wet and dry spells are different in wet and dry seasons, and that the increases in dry spell lengths expected under future climate change mostly occur during the annual dry seasons. This has important implications for agriculture across the tropics, and suggests that crops grown solely during the wet season may be less affected by longer dry spells and increased water stress. However, for crops grown during the dry season and perennial crops, longer dry spells in the dry season, combined with lower dry season rainfall and fewer dry season rainy days may lead to elevated dry season water stress. This elevated dry season water stress will be further exacerbated by increased evaporative demand due to higher temperatures; Scheff and Frierson (2015) found aridification generally dominates over humidification in the tropics and subtropics due to temperature-driven increases in potential evapotranspiration. Regions such as central America, north-east South America, Southern Africa and Australia will be most impacted by this. Further work, using detailed crop models, is required to determine the impacts on individual crops.

Regional variations in the response of wet and dry spells to elevated greenhouse gas concentrations have been identified; the aim of this paper is to assess the changes in wet/dry season precipitation characteristics and not to understand the regional changes in terms of circulation change. Regional changes in rainfall across the tropics are driven by a range of factors including changes in the Intertropical Convergence Zone (contraction, intensification and timing; Dwyer et al. 2014; Su et al. 2017; Song et al. 2018) and subtropical drying, which is determined by complex interplay between Hadley Cell expansion (Seidel et al. 2008; Scheff and Frierson 2012), land ocean warming contrasts (Karnauskas and Ummenhofer 2014; He and Soden 2017), and

vegetation responses to elevated CO_2 (Mankin et al. 2018). Further work is required to understand the changing regional/local circulations and energy and water fluxes that lead to these changes over different regions.

Acknowledgments. We would like to thank Salvatore Pascale and two anonymous reviewers for their insightful and constructive reviews.

We acknowledge the World Climate Research Programme, which, through its Working Group on Coupled Modelling, coordinated and promoted CMIP6. We thank the climate modeling groups (Table S1 and S2) for producing and making available their model output, the Earth System Grid Federation (ESGF) for archiving the data and providing access, and the multiple funding agencies who support CMIP6 and ESGF. For CMIP5 the U.S. Department of Energy's Program for Climate Model Diagnosis and Intercomparison provides coordinating support and led development of software infrastructure in partnership with the Global Organization for Earth System Science Portals.

Emily Black was supported by the National Centre for Atmospheric Science via the NERC/GCRF programme Atmospheric hazard in developing countries: risk assessment and early warning (ACREW). Emily Black also gratefully acknowledges support from the Global Challenges Research Fund project, SatWIN-ALERT(NE/R014116/1). Richard P. Allan was funded by the National Centre for Earth Observation grant NE/RO16518/1. We are grateful to the Mars Wrigley Confectionery research team for stimulating discussions on the wider context and applications of this work.

Data availability statement. CHIRPS rainfall data are available from `https://data.chc.ucsb.edu/products/CHIRPS-2.0/`. CMIP5 and CMIP6 data were obtained from the British Atmospheric Data Centre (BADC) hosted at the Centre for Environmental Data Analysis (CEDA).

References

Aadhar, S., and V. Mishra, 2020: On the Projected Decline in Droughts Over South Asia in CMIP6 Multimodel Ensemble. *Journal of Geophysical Research: Atmospheres*, **125 (20)**, e2020JD033 587, doi:https://doi.org/10.1029/2020JD033587.

Allan, R. P., and Coauthors, 2020: Advances in understanding large-scale responses of the water cycle to climate change. *Annals of the New York Academy of Sciences*, **1472 (1)**, 49–75.

Allen, M. R., and W. J. Ingram, 2002: Constraints on future changes in climate and the hydrologic cycle. *Nature*, **419 (6903)**, 228–232.

Avila-Diaz, A., V. Benezoli, F. Justino, R. Torres, and A. Wilson, 2020: Assessing current and future trends of climate extremes across Brazil based on reanalyses and earth system model projections. *Climate Dynamics*, **55 (5)**, 1403–1426.

Barkhordarian, A., H. von Storch, A. Behrangi, P. C. Loikith, C. R. Mechoso, and J. Detzer, 2018: Simultaneous Regional Detection of Land-Use Changes and Elevated GHG Levels: The Case of Spring Precipitation in Tropical South America. *Geophysical Research Letters*, **45 (12)**, 6262–6271.

Beck, H. E., E. F. Wood, M. Pan, C. K. Fisher, D. G. Miralles, A. I. J. M. van Dijk, T. R. McVicar, and R. F. Adler, 2019: MSWEP V2 Global 3-Hourly 0.1° Precipitation: Methodology and Quantitative Assessment. *Bulletin of the American Meteorological Society*, **100 (3)**, 473 – 500.

Biasutti, M., and A. H. Sobel, 2009: Delayed Sahel rainfall and global seasonal cycle in a warmer climate. *Geophysical Research Letters*, **36 (23)**, L23 707.

Brogli, R., S. L. Sørland, N. Kröner, and C. Schär, 2019: Causes of future Mediterranean precipitation decline depend on the season. *Environmental Research Letters*, **14 (11)**, 114 017.

Chou, C., J. C. H. Chiang, C.-W. Lan, C.-H. Chung, Y.-C. Liao, and C.-J. Lee, 2013: Increase in the range between wet and dry season precipitation. *Nature Geoscience*, **6 (4)**, 263–267.

Collins, M., and Coauthors, 2013: Long-term climate change: projections, commitments and irreversibility. *Climate Change 2013-The Physical Science Basis: Contribution of Working Group I to the Fifth Assessment Report of the Intergovernmental Panel on Climate Change*, Cambridge University Press, 1029–1136.

Correa, I. C., P. A. Arias, and M. Rojas, 2020: Evaluation of multiple indices of the South American monsoon. *International Journal of Climatology*, **41 (S1)**, E2801–E2819.

Creese, A., and R. Washington, 2018: A process-based assessment of CMIP5 rainfall in the Congo Basin: the September–November rainy season. *Journal of Climate*, **31 (18)**, 7417–7439.

Dai, A., T. Zhao, and J. Chen, 2018: Climate change and drought: A precipitation and evaporation perspective. *Current Climate Change Reports*, **4 (3)**, 301–312.

Deng, S., C. Sheng, N. Yang, L. Song, and Q. Huang, 2020: Anthropogenic forcing enhances rainfall seasonality in global land monsoon regions. *Environmental Research Letters*, **15 (10)**, 104 057.

Dong, G., Z. Jiang, Z. Tian, E. Buonomo, L. Sun, and D. Fan, 2020: Projecting Changes in Mean and Extreme Precipitation Over Eastern China During 2041–2060. *Earth and Space Science*, **7 (9)**, e2019EA001 024.

Dunning, C. M., R. P. Allan, and E. Black, 2017: Identification of deficiencies in seasonal rainfall simulated by CMIP5 climate models. *Environmental Research Letters*, **12 (11)**, 114 001.

Dunning, C. M., E. Black, and R. P. Allan, 2018: Later wet seasons with more intense rainfall over Africa under future climate change. *Journal of Climate*, **31 (23)**, 9719–9738.

738 Dunning, C. M., E. C. Black, and R. P. Allan, 2016: The onset and cessation of seasonal rainfall
739 over Africa. *Journal of Geophysical Research: Atmospheres*, **121 (19)**, 11,405– 11,424.

740 Dwyer, J. G., M. Biasutti, and A. H. Sobel, 2014: The Effect of Greenhouse Gas–Induced Changes
741 in SST on the Annual Cycle of Zonal Mean Tropical Precipitation. *Journal of Climate*, **27 (12)**,
742 4544–4565.

743 Eekhout, J. P. C., J. E. Hunink, W. Terink, and J. de Vente, 2018: Why increased extreme
744 precipitation under climate change negatively affects water security. *Hydrology and Earth System*
745 *Sciences*, **22 (11)**, 5935–5946.

746 Espinoza, J. C., J. Ronchail, J. A. Marengo, and H. Segura, 2019: Contrasting North–South
747 changes in Amazon wet-day and dry-day frequency and related atmospheric features (1981–
748 2017). *Climate Dynamics*, **52 (9-10)**, 5413–5430.

749 Eyring, V., S. Bony, G. A. Meehl, C. A. Senior, B. Stevens, R. J. Stouffer, and K. E. Taylor, 2016:
750 Overview of the Coupled Model Intercomparison Project Phase 6 (CMIP6) experimental design
751 and organization. *Geoscientific Model Development*, **9 (5)**, 1937–1958.

752 FAO, 2020: Crop information: Sorghum (accessed 2020-12-01). URL http://www.fao.org/
753 land-water/databases-and-software/crop-information/sorghum/en/.

754 Feng, X., A. Porporato, and I. Rodriguez-Iturbe, 2013: Changes in rainfall seasonality in the
755 tropics. *Nature Climate Change*, **3 (9)**, 811–815.

756 Funk, C., L. Harrison, L. Alexander, P. Peterson, A. Behrangi, and G. Husak, 2019: Exploring
757 trends in wet-season precipitation and drought indices in wet, humid and dry regions. *Environ-*
758 *mental Research Letters*, **14 (11)**, 115 002.

Funk, C., and Coauthors, 2015: The climate hazards infrared precipitation with stations—a new environmental record for monitoring extremes. *Scientific Data*, **2 (1)**, 1–21.

Ge, F., and Coauthors, 2019: Risks of precipitation extremes over Southeast Asia: does 1.5° C or 2° C global warming make a difference? *Environmental Research Letters*, **14 (4)**, 044 015.

Giorgi, F., E. Coppola, and F. Raffaele, 2014: A consistent picture of the hydroclimatic response to global warming from multiple indices: Models and observations. *Journal of Geophysical Research: Atmospheres*, **119 (20)**, 11 695–11 708.

Giorgi, F., E.-S. Im, E. Coppola, N. Diffenbaugh, X. Gao, L. Mariotti, and Y. Shi, 2011: Higher hydroclimatic intensity with global warming. *Journal of Climate*, **24 (20)**, 5309–5324.

Giorgi, F., F. Raffaele, and E. Coppola, 2019: The response of precipitation characteristics to global warming from climate projections. *Earth System Dynamics*, **10 (1)**, 73–89.

Gudoshava, M., and Coauthors, 2020: Projected effects of 1.5 C and 2 C global warming levels on the intra-seasonal rainfall characteristics over the Greater Horn of Africa. *Environmental Research Letters*, **15 (3)**, 034 037.

Ha, K.-J., S. Moon, A. Timmermann, and D. Kim, 2020: Future changes of summer monsoon characteristics and evaporative demand over Asia in CMIP6 simulations. *Geophysical Research Letters*, **47 (8)**, e2020GL087 492.

Han, T., H. Chen, X. Hao, and H. Wang, 2018: Projected changes in temperature and precipitation extremes over the Silk Road Economic Belt regions by the Coupled Model Intercomparison Project Phase 5 multi-model ensembles. *International Journal of Climatology*, **38 (11)**, 4077–4091.

He, C., T. Li, and W. Zhou, 2020: Drier North American Monsoon in Contrast to Asian–African Monsoon under Global Warming. *Journal of Climate*, **33 (22)**, 9801–9816.

He, J., and B. J. Soden, 2017: A re-examination of the projected subtropical precipitation decline. *Nature Climate Change*, **7 (1)**, 53–57.

Held, I. M., and B. J. Soden, 2006: Robust Responses of the Hydrological Cycle to Global Warming. *Journal of Climate*, **19 (21)**, 5686–5699.

Herrmann, S. M., and K. I. Mohr, 2011: A continental-scale classification of rainfall seasonality regimes in Africa based on gridded precipitation and land surface temperature products. *Journal of Applied Meteorology and Climatology*, **50 (12)**, 2504–2513.

Iturbide, M., and Coauthors, 2020: An update of IPCC climate reference regions for subcontinental analysis of climate model data: Definition and aggregated datasets. *Earth System Science Data*, **12 (4)**, 2959–2970.

Karnauskas, K. B., and C. C. Ummenhofer, 2014: On the dynamics of the Hadley circulation and subtropical drying. *Climate Dynamics*, **42 (9-10)**, 2259–2269.

Kitoh, A., H. Endo, K. Krishna Kumar, I. F. Cavalcanti, P. Goswami, and T. Zhou, 2013: Monsoons in a changing world: a regional perspective in a global context. *Journal of Geophysical Research: Atmospheres*, **118 (8)**, 3053–3065.

Klutse, N. A. B., and Coauthors, 2018: Potential impact of 1.5 C and 2 C global warming on consecutive dry and wet days over West Africa. *Environmental Research Letters*, **13 (5)**, 055 013.

Kooperman, G. J., M. D. Fowler, F. M. Hoffman, C. D. Koven, K. Lindsay, M. S. Pritchard, A. L. Swann, and J. T. Randerson, 2018: Plant physiological responses to rising CO_2 modify simulated

daily runoff intensity with implications for global-scale flood risk assessment. *Geophysical Research Letters*, **45 (22)**, 12–457.

Kumar, S., R. P. Allan, F. Zwiers, D. M. Lawrence, and P. A. Dirmeyer, 2015: Revisiting trends in wetness and dryness in the presence of internal climate variability and water limitations over land. *Geophysical Research Letters*, **42 (24)**, 10,867–10,875.

Lan, C.-W., M.-H. Lo, C.-A. Chen, and J.-Y. Yu, 2019: The mechanisms behind changes in the seasonality of global precipitation found in reanalysis products and CMIP5 simulations. *Climate Dynamics*, **53 (7-8)**, 4173–4187.

Lau, W. K.-M., H.-T. Wu, and K.-M. Kim, 2013: A canonical response of precipitation characteristics to global warming from CMIP5 models. *Geophysical Research Letters*, **40 (12)**, 3163–3169.

Liebmann, B., I. Bladé, G. N. Kiladis, L. M. Carvalho, G. B. Senay, D. Allured, S. Leroux, and C. Funk, 2012: Seasonality of African precipitation from 1996 to 2009. *Journal of Climate*, **25 (12)**, 4304–4322.

Mankin, J. S., R. Seager, J. E. Smerdon, B. I. Cook, and A. P. Williams, 2019: Mid-latitude freshwater availability reduced by projected vegetation responses to climate change. *Nature Geoscience*, **12 (12)**, 983–988.

Mankin, J. S., R. Seager, J. E. Smerdon, B. I. Cook, A. P. Williams, and R. M. Horton, 2018: Blue water trade-offs with vegetation in a CO2-enriched climate. *Geophysical Research Letters*, **45 (7)**, 3115–3125.

Marvel, K., M. Biasutti, C. Bonfils, K. E. Taylor, Y. Kushnir, and B. I. Cook, 2017: Observed and Projected Changes to the Precipitation Annual Cycle. *Journal of Climate*, **30 (13)**, 4983–4995.

824 Mba, W. P., and Coauthors, 2018: Consequences of 1.5 C and 2 C global warming levels for
825 temperature and precipitation changes over Central Africa. *Environmental Research Letters*,
826 **13 (5)**, 055 011.

827 Meehl, G. A., C. A. Senior, V. Eyring, G. Flato, J.-F. Lamarque, R. J. Stouffer, K. E. Taylor, and
828 M. Schlund, 2020: Context for interpreting equilibrium climate sensitivity and transient climate
829 response from the CMIP6 Earth system models. *Science Advances*, **6 (26)**, eaba1981.

830 Ogega, O. M., J. Koske, J. B. Kung'u, E. Scoccimarro, H. S. Endris, and M. N. Mistry, 2020:
831 Heavy precipitation events over East Africa in a changing climate: results from CORDEX
832 RCMs. *Climate Dynamics*, **55**, 993–1009.

833 O'Neill, B. C., and Coauthors, 2016: The Scenario Model Intercomparison Project (ScenarioMIP)
834 for CMIP6. *Geoscientific Model Development*, **9 (9)**, 3461–3482.

835 Orlowsky, B., and S. I. Seneviratne, 2012: Global changes in extreme events: regional and seasonal
836 dimension. *Climatic Change*, **110 (3-4)**, 669–696.

837 Osima, S., and Coauthors, 2018: Projected climate over the Greater Horn of Africa under 1.5 C
838 and 2 C global warming. *Environmental Research Letters*, **13 (6)**, 065 004.

839 Parsons, L., 2020: Implications of CMIP6 projected drying trends for 21st century Amazonian
840 drought risk. *Earth's Future*, **8 (10)**, e2020EF001 608.

841 Pascale, S., V. Lucarini, X. Feng, A. Porporato, and S. ul Hasson, 2016: Projected changes
842 of rainfall seasonality and dry spells in a high greenhouse gas emissions scenario. *Climate*
843 *Dynamics*, 1410.3116.

844 Peters, W., and Coauthors, 2018: Increased water-use efficiency and reduced CO_2 uptake by plants
845 during droughts at a continental scale. *Nature Geoscience*, **11 (10)**, 744–748.

Pinto, I., C. Lennard, M. Tadross, B. Hewitson, A. Dosio, G. Nikulin, H.-J. Panitz, and M. E. Shongwe, 2016: Evaluation and projections of extreme precipitation over southern Africa from two CORDEX models. *Climatic Change*, **135 (3-4)**, 655–668.

Polade, S. D., D. W. Pierce, D. R. Cayan, A. Gershunov, and M. D. Dettinger, 2014: The key role of dry days in changing regional climate and precipitation regimes. *Scientific Reports*, **4**, 4364.

Polson, D., and G. Hegerl, 2017: Strengthening contrast between precipitation in tropical wet and dry regions. *Geophysical Research Letters*, **44 (1)**, 365–373.

Richardson, T., and Coauthors, 2018: Carbon dioxide physiological forcing dominates projected eastern Amazonian drying. *Geophysical Research Letters*, **45 (6)**, 2815–2825.

Rockström, J., and Coauthors, 2010: Managing water in rainfed agriculture—The need for a paradigm shift. *Agricultural Water Management*, **97 (4)**, 543–550.

Rowell, D. P., B. B. Booth, S. E. Nicholson, and P. Good, 2015: Reconciling past and future rainfall trends over East Africa. *Journal of Climate*, **28 (24)**, 9768–9788.

Scheff, J., and D. M. Frierson, 2012: Robust future precipitation declines in CMIP5 largely reflect the poleward expansion of model subtropical dry zones. *Geophysical Research Letters*, **39**, L18 704.

Scheff, J., and D. M. Frierson, 2015: Terrestrial aridity and its response to greenhouse warming across CMIP5 climate models. *Journal of Climate*, **28 (14)**, 5583–5600.

Schurer, A. P., A. P. Ballinger, A. R. Friedman, and G. C. Hegerl, 2020: Human influence strengthens the contrast between tropical wet and dry regions. *Environmental Research Letters*, **15 (10)**, 104 026.

867 Schwalm, C. R., S. Glendon, and P. B. Duffy, 2020: RCP8.5 tracks cumulative CO2 emissions.
868 *Proceedings of the National Academy of Sciences*, **117 (33)**, 19 656–19 657.

869 Seidel, D. J., Q. Fu, W. J. Randel, and T. J. Reichler, 2008: Widening of the tropical belt in a
870 changing climate. *Nature Geoscience*, **1 (1)**, 21–24.

871 Seneviratne, S., and Coauthors, 2012: Changes in climate extremes and their impacts on the natural
872 physical environment. *Managing the risks of extreme events and disasters to advance climate*
873 *change adaptation*, A Special Report of Working Groups I and II of the Intergovernmental Panel
874 on Climate Change (IPCC). Cambridge University Press Cambridge, UK, and New York, NY,
875 USA, 109–230.

876 Seth, A., S. A. Rauscher, M. Biasutti, A. Giannini, S. J. Camargo, and M. Rojas, 2013: CMIP5
877 Projected Changes in the Annual Cycle of Precipitation in Monsoon Regions. *Journal of Climate*,
878 **26 (19)**, 7328–7351.

879 Sillmann, J., V. Kharin, X. Zhang, F. Zwiers, and D. Bronaugh, 2013a: Climate extremes indices
880 in the CMIP5 multimodel ensemble: Part 1. Model evaluation in the present climate. *Journal of*
881 *Geophysical Research: Atmospheres*, **118 (4)**, 1716–1733.

882 Sillmann, J., V. V. Kharin, F. Zwiers, X. Zhang, and D. Bronaugh, 2013b: Climate extremes indices
883 in the CMIP5 multimodel ensemble: Part 2. Future climate projections. *Journal of Geophysical*
884 *Research: Atmospheres*, **118 (6)**, 2473–2493.

885 Small, R. J. O., S. P. de Szoeke, and S.-P. Xie, 2007: The Central American Midsummer Drought:
886 Regional Aspects and Large-Scale Forcing. *Journal of Climate*, **20 (19)**, 4853 – 4873.

887 Song, F., L. R. Leung, J. Lu, and L. Dong, 2018: Seasonally dependent responses of subtropical
888 highs and tropical rainfall to anthropogenic warming. *Nature Climate Change*, **8 (9)**, 787–792.

Su, H., and Coauthors, 2017: Tightening of tropical ascent and high clouds key to precipitation change in a warmer climate. *Nature Communications*, **8**, 15 771.

Taylor, K. E., R. J. Stouffer, and G. A. Meehl, 2012: An overview of CMIP5 and the experiment design. *Bulletin of the American Meteorological Society*, **93 (4)**, 485–498.

Tegegne, G., A. M. Melesse, and T. Alamirew, 2020: Projected changes in extreme precipitation indices from CORDEX simulations over Ethiopia, East Africa. *Atmospheric Research*, **247**, 105 156.

Trenberth, K. E., 2011: Changes in precipitation with climate change. *Climate Research*, **47 (1-2)**, 123–138.

Van Vuuren, D. P., and Coauthors, 2011: The representative concentration pathways: an overview. *Climatic Change*, **109 (1-2)**, 5.

Wang, B., C. Jin, and J. Liu, 2020: Understanding future change of global monsoons projected by CMIP6 models. *Journal of Climate*, **33 (15)**, 6471–6489.

Wang, B., and Coauthors, 2021: Monsoons climate change assessment. *Bulletin of the American Meteorological Society*, **102 (1)**, E1–E19.

Yang, W., R. Seager, M. A. Cane, and B. Lyon, 2015: The Annual Cycle of East African Precipitation. *Journal of Climate*, **28 (6)**, 2385–2404.

Yin, J., P. Gentine, S. Zhou, S. C. Sullivan, R. Wang, Y. Zhang, and S. Guo, 2018: Large increase in global storm runoff extremes driven by climate and anthropogenic changes. *Nature Communications*, **9 (1)**, 1–10.

Zhang, X., L. Alexander, G. C. Hegerl, P. Jones, A. K. Tank, T. C. Peterson, B. Trewin, and F. W. Zwiers, 2011: Indices for monitoring changes in extremes based on daily temperature and precipitation data. *Wiley Interdisciplinary Reviews: Climate Change*, **2 (6)**, 851–870.

Zhao, T., and A. Dai, 2015: The magnitude and causes of global drought changes in the twenty-first century under a low–moderate emissions scenario. *Journal of climate*, **28 (11)**, 4490–4512.

Zhou, L., H. Chen, and Y. Dai, 2015: Stronger warming amplification over drier ecoregions observed since 1979. *Environmental Research Letters*, **10 (6)**, 064 012.

LIST OF FIGURES

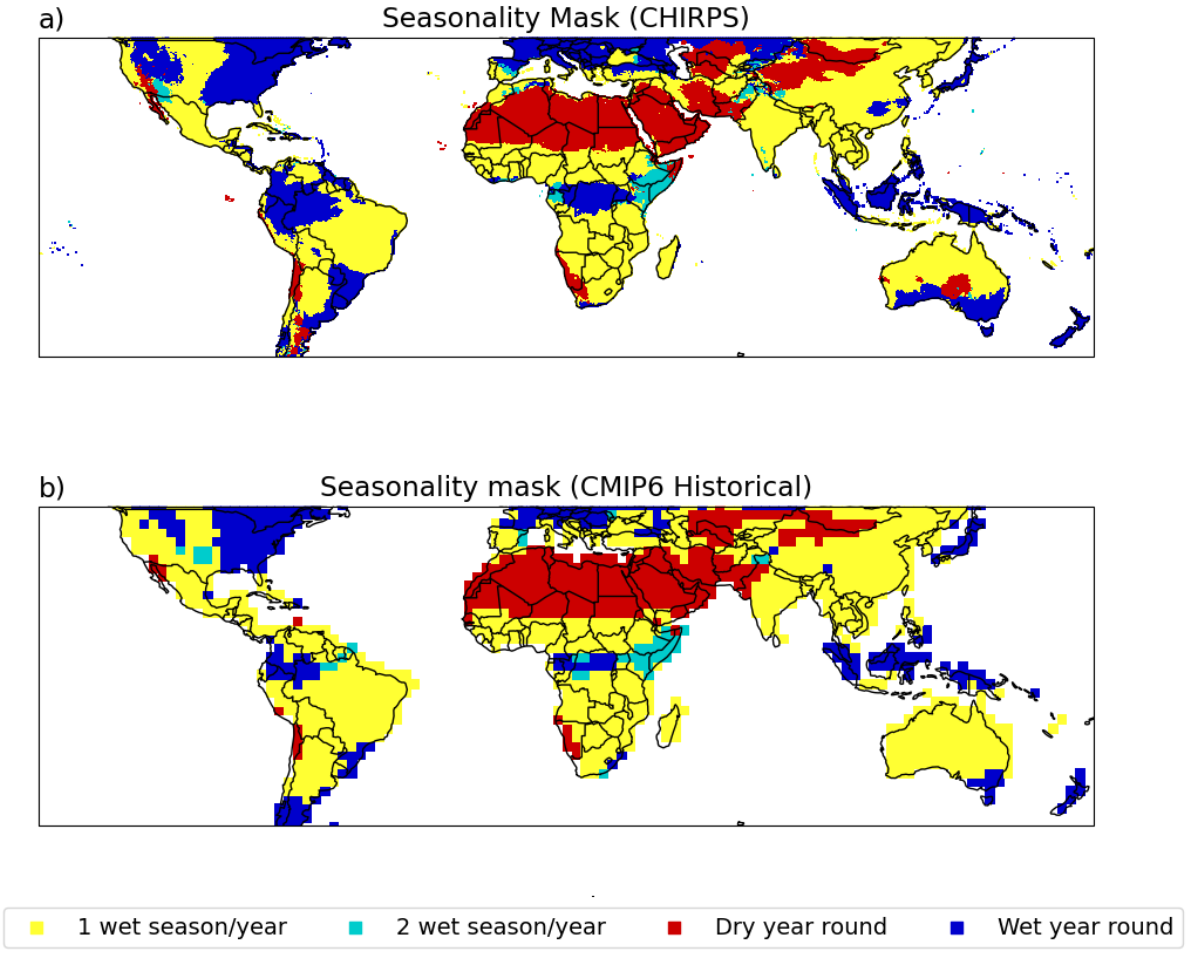

1002 FIG. 1. a) Seasonality mask produced using CHIRPS rainfall data over 1985-2014. b) CMIP6 multi-model
1003 modal seasonality mask for the historical simulation over 1985-2014. Red indicates dry-year-round, blue indicates
1004 wet-year-round, yellow indicates one wet season per year and green indicates two wet seasons per year. See
1005 Figure S1 for CMIP5 and other scenarios.

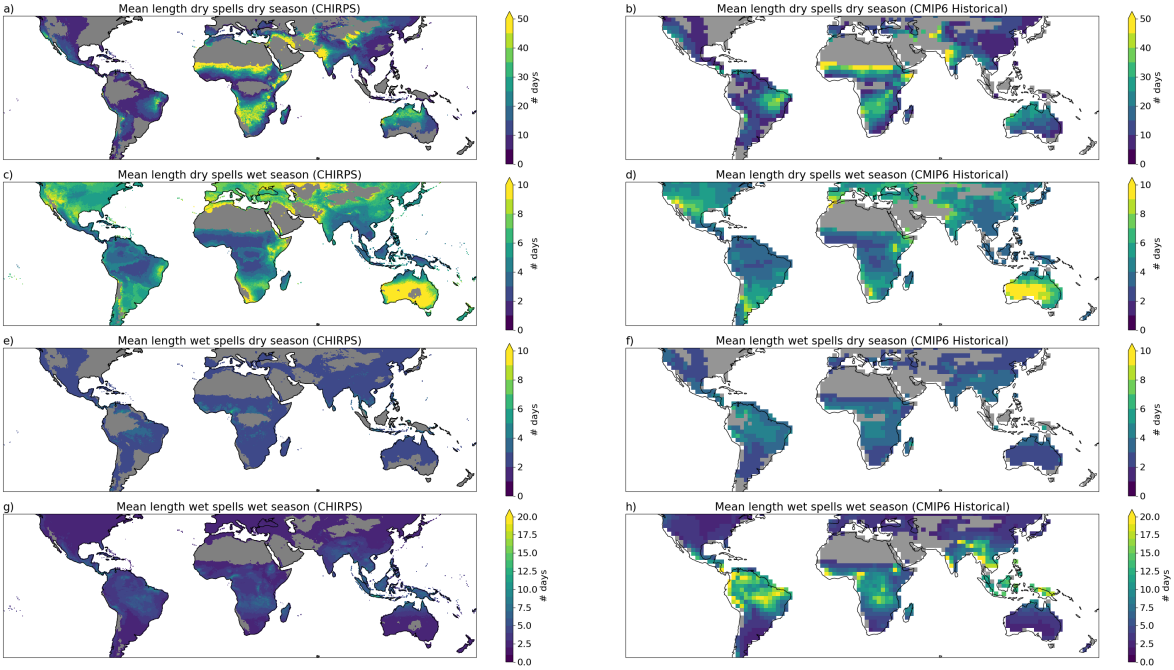

FIG. 2. Mean length of a-b) dry spells in the dry season, c-d) dry spells in the wet season, e-f) wet spells in the dry season and g-h) wet spells in the wet season from CHIRPS (a,c,e,g) and the multi-model median of the CMIP6 historical simulations (b,d,f,h). 1985-2014 is used for both CHIRPS and CMIP6. Grey regions indicate where at least 50% of the models do not give a value (dry year round or wet year round in the dry season plots), or where CHIRPS is wet year round or dry year round.

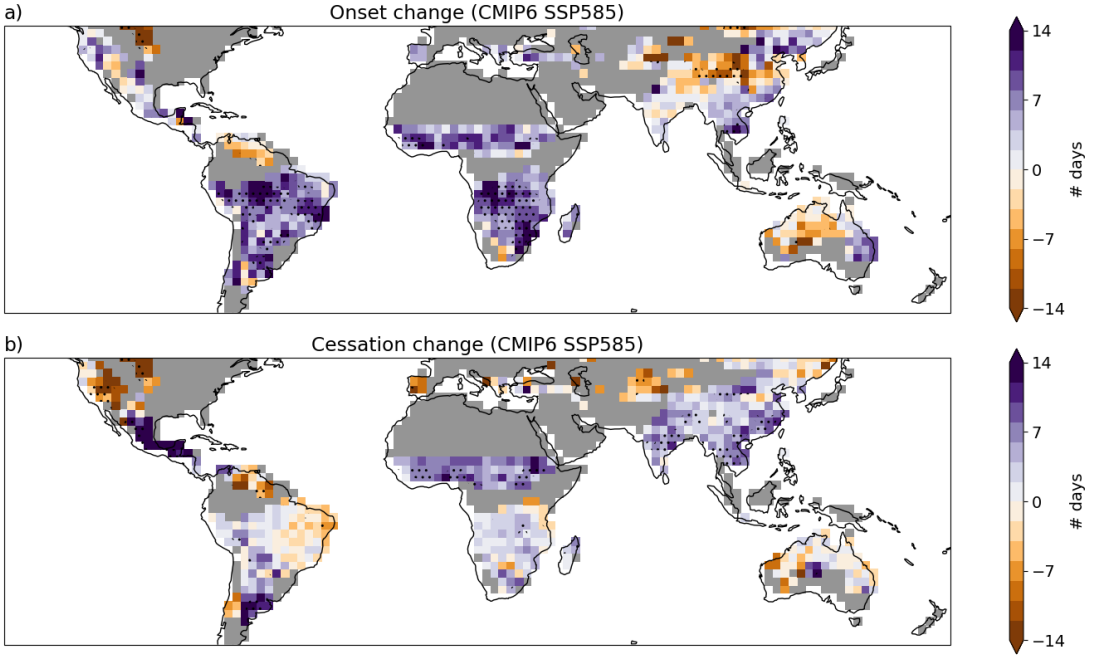

FIG. 3. CMIP6 multi-model median change in a) onset of the annual wet season and b) cessation of the annual wet season for the SSP585 scenario over 2070-2099 compared with the historical simulation over 1985-2014. Purple indicates later while orange indicates earlier. Stippling indicates where 75% of the models agree on the sign of the median. Grey regions indicate where at least 50% of the models do not give a value (dry year round/wet year round/ biannual regime).

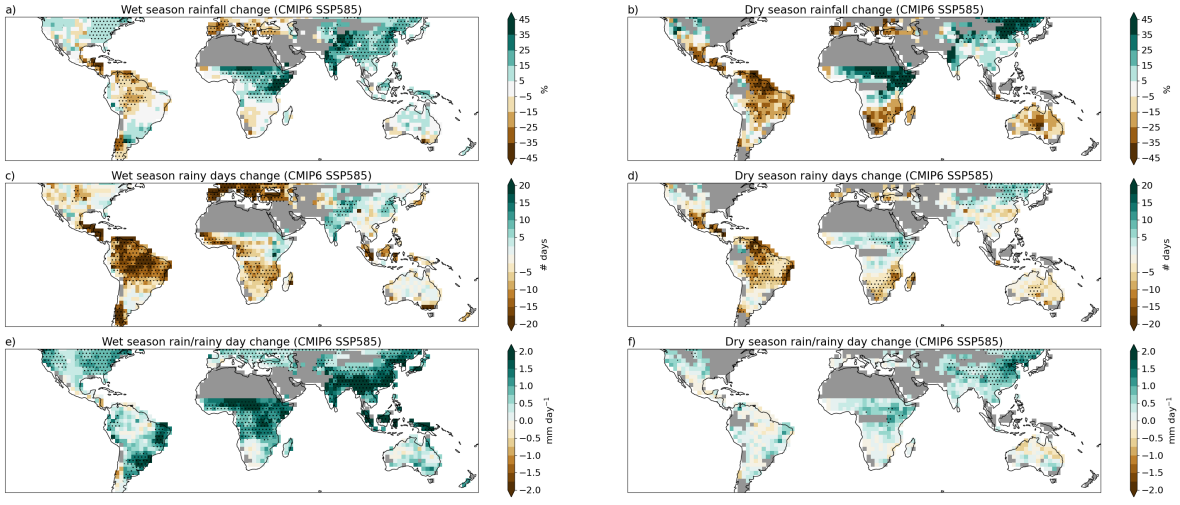

FIG. 4. CMIP6 multi-model median change in a) wet season rainfall, b) dry season rainfall, c) number of rainy days in the wet season, d) number of rainy days in the dry season, e) wet season rain per rainy day and f) dry season rain per rainy day for the SSP585 scenario over 2070-2099 compared with the historical simulation over 1985-2014. Stippling indicates where 60% of the models show a statistically significant change (t-test, 10% significance level) of the same sign as the median change. Grey regions indicate where at least 50% of the models do not give a value (dry year round or wet year round in the dry season plots).

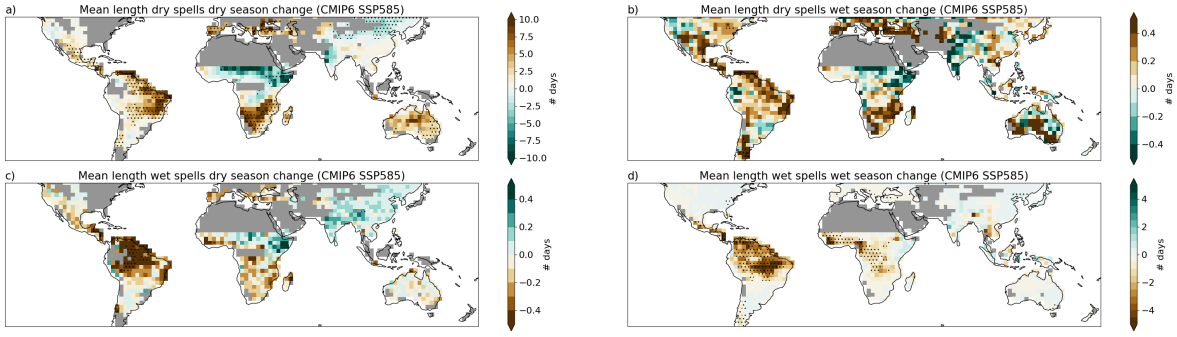

1022 FIG. 5. CMIP6 multi-model median change in a) mean length of dry spells in the dry season, b) mean length
1023 of dry spells in the wet season, c) mean length of wet spells in the dry season, and d) mean length of wet spells in
1024 the wet season for the SSP585 scenario over 2070-2099 compared with the historical simulation over 1985-2014.
1025 Stippling indicates where 60% of the models show a statistically significant change (t-test, 10% significance
1026 level) of the same sign as the median change. Grey regions indicate where at least 50% of the models do not give
1027 a value (dry year round or wet year round in the dry season plots).

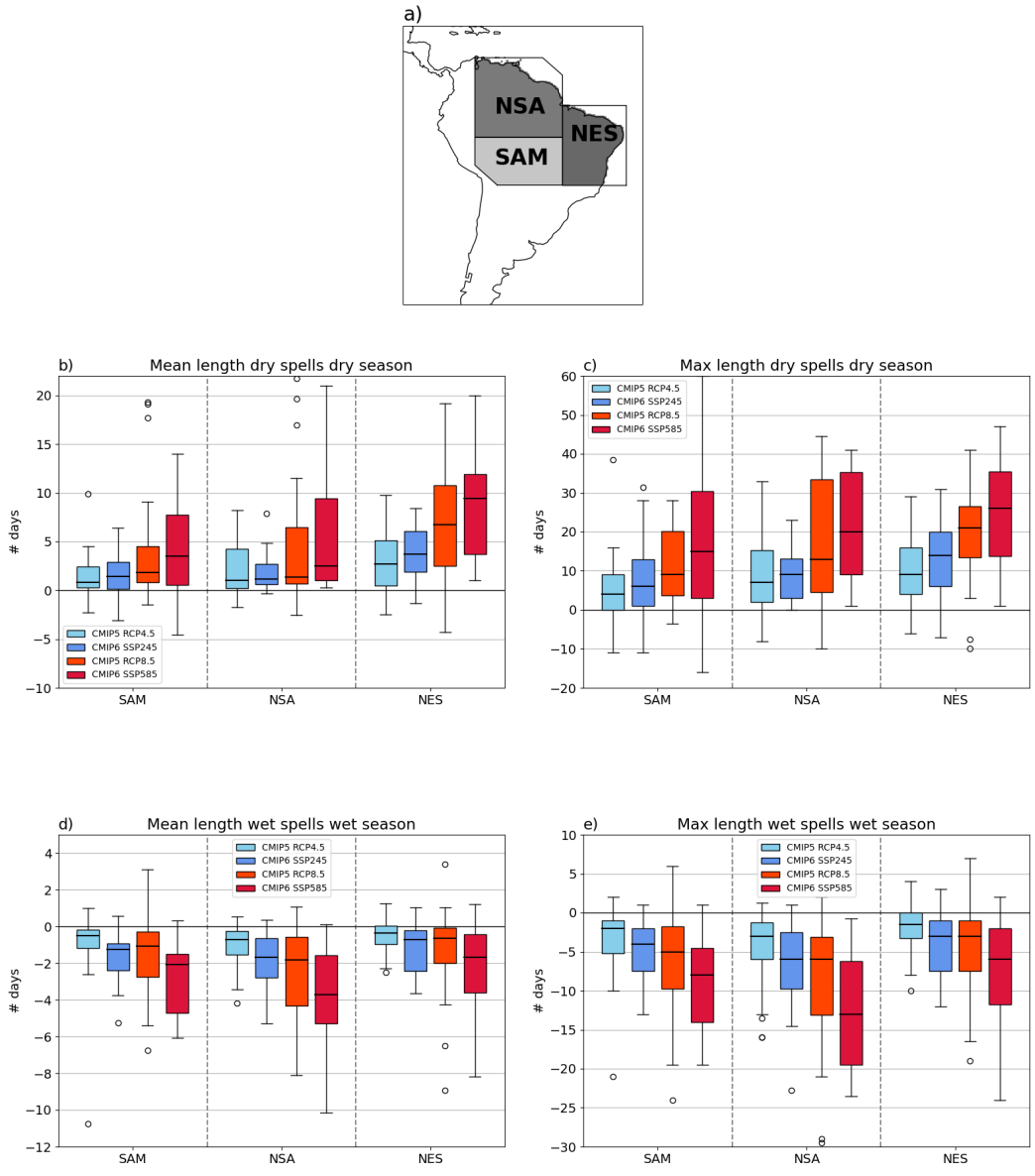

FIG. 6. a) Region map showing the location of South American Monsoon (SAM), north South America (NSA) and north-east South America (NES). b-c) Boxplots showing the change in mean/max length of dry spells in the dry season and d-e) boxplots showing the change in mean/max length of wet spells in the wet season over SAM, NSA, and NES. The different colours indicate the CMIP era (CMIP5 or CMIP6) and scenario (SSP 245, SSP 585, RCP 4.5, RCP 8.5). For all boxplots the change is computed from the historical simulation for 1985-2014 to the select scenario for 2070-2099. The box extends from the lower quartile (Q1) to the upper quartile (Q3) of the data and the line in the middle shows the median. The whiskers extend from the first datum greater than Q1 minus 1.5 times the interquartile range to the last datum less than Q3 plus 1.5 times the interquartile range - values outside this range are considered to be outliers and marked with a circle. The same is the case for all boxplots in this paper.

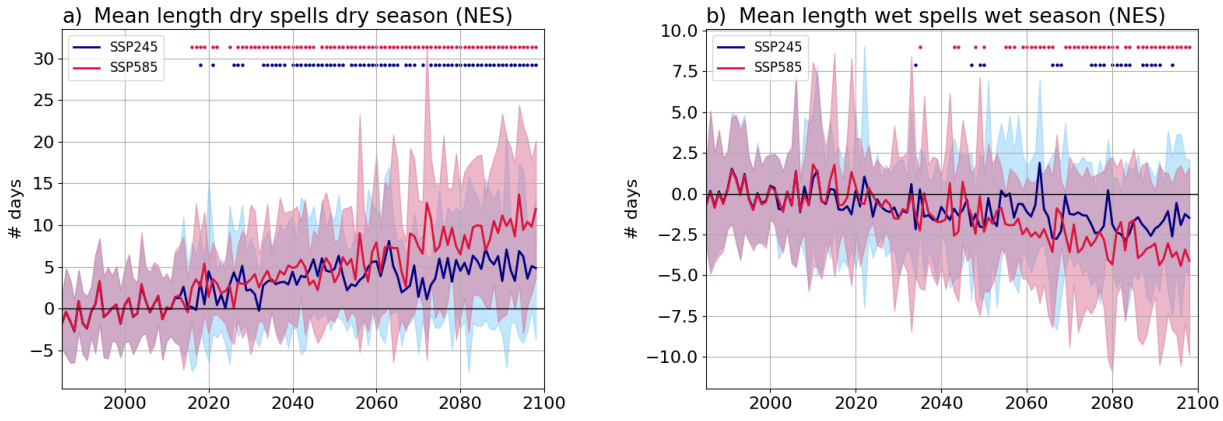

FIG. 7. Timeseries of a) mean length of dry spells in the dry season and b) mean length of wet spells in the wet season for the north-east South America region. The blue/red line shows the multi-model mean over the CMIP6 models for the SSP245/SSP585 scenario; the shading indicates one standard deviation. The dots indicate when the range of values from 18 models for that year is significantly different from the range for 1985–2014 at the 5% level, using a Mann–Whitney U and t test.

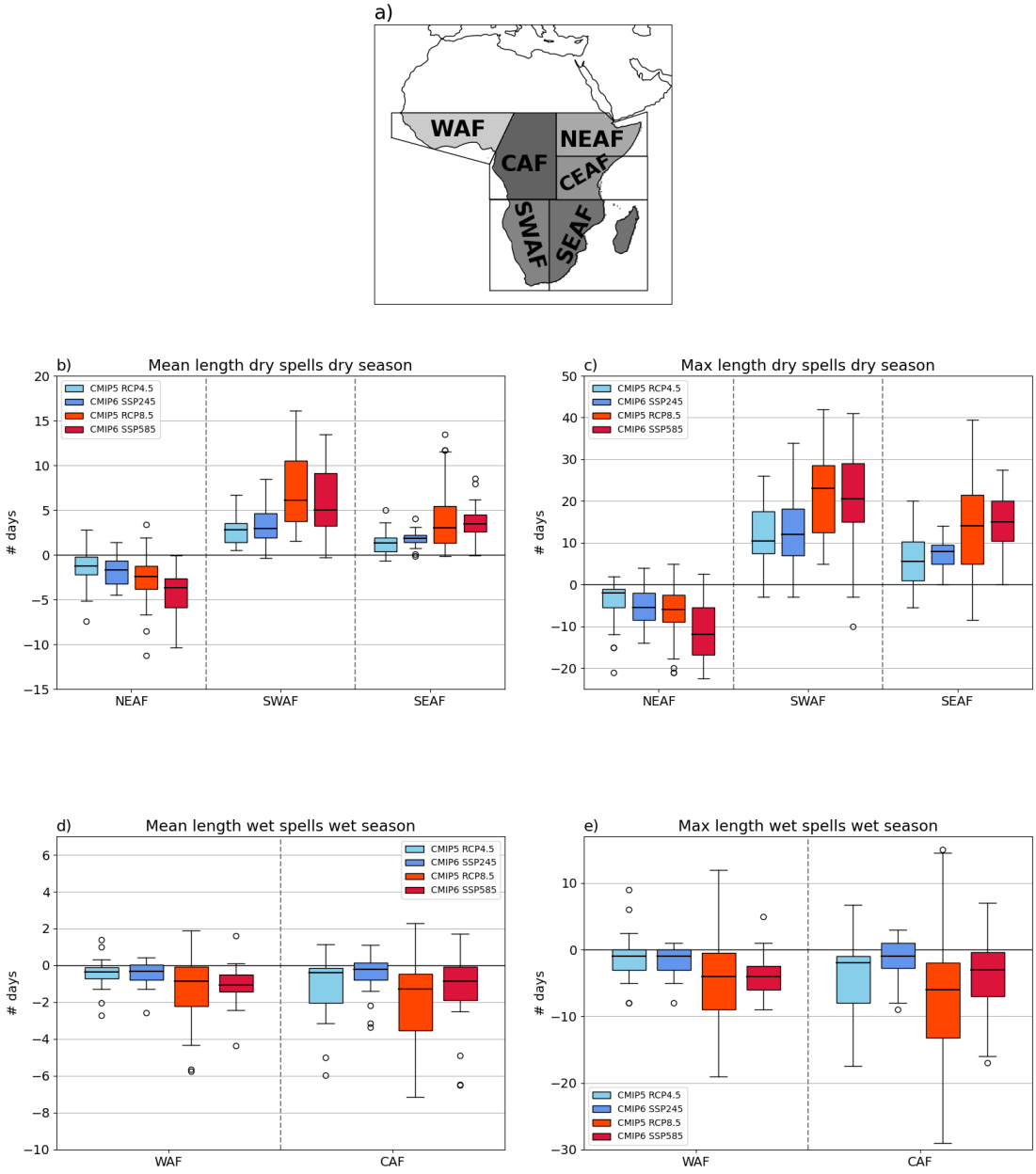

FIG. 8. a) Region map showing the location of West Africa (WAF), Central Africa (CAF), North East Africa (NEAF), Central East Africa (CEAF), South West Africa (SWAF), and South East Africa (SEAF). b-c) Boxplots showing the change in mean/max length of dry spells in the dry season over NEAF, SWAF and SEAF. d-e) Boxplots showing mean/max length of wet spells in the wet season over WAF and CAF. The different colours indicate the CMIP era (CMIP5 or CMIP6) and scenario (SSP 245, SSP 585, RCP 4.5, RCP 8.5). For all boxplots the change is computed from the historical simulation for 1985-2014 to the select scenario for 2070-2099. Results for all regions are shown in Figure S17.

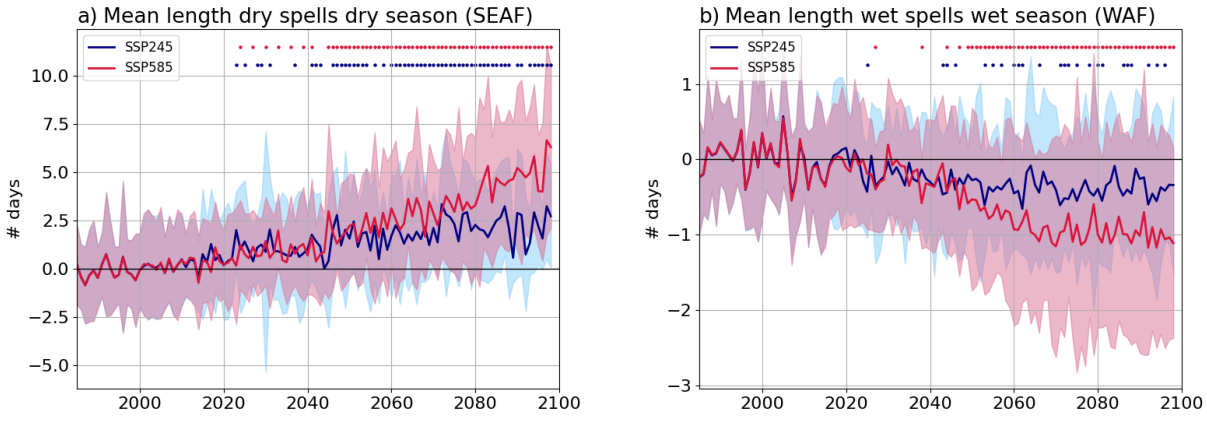

FIG. 9. Timeseries of a) mean length of dry spells in the dry season over south-east Africa (SEAF) and b) mean length of wet spells in the wet season over West Africa (WAF). The blue/red line shows the multi-model mean over the CMIP6 models for the SSP245/SSP585 scenario; the shading indicates one standard deviation. The dots indicate when the range of values from 18 models for that year is significantly different from the range for 1985–2014 at the 5% level, using a Mann–Whitney U and t test.

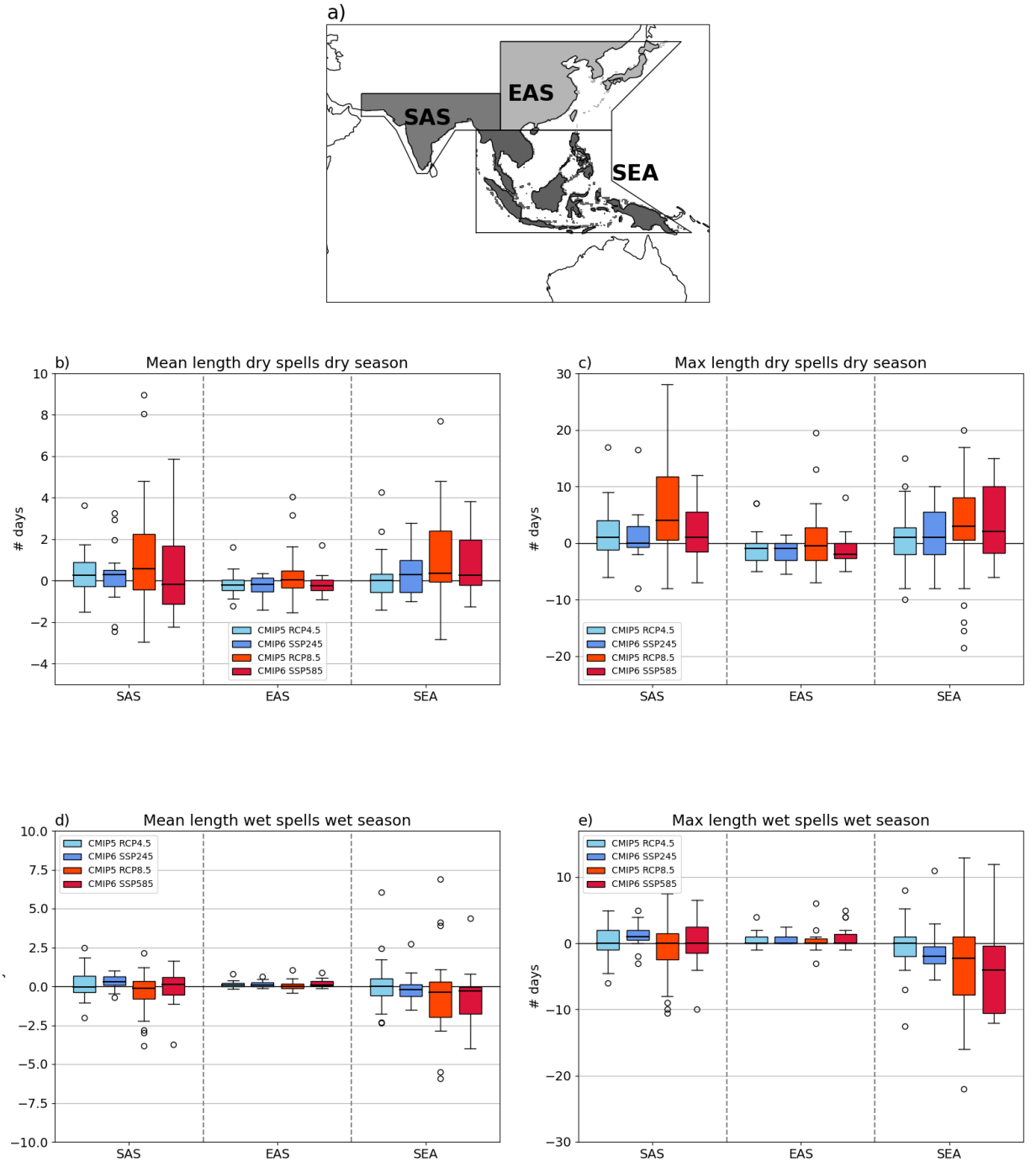

FIG. 10. a) Region map showing the location of South Asia (SAS), East Asia (EAS), and South East Asia (SEA). b-c) Boxplots showing the change in mean/max length of dry spells in the dry season. d-e) Boxplots showing the change in mean/max length of wet spells in the wet season. The different colours indicate the CMIP era (CMIP5 or CMIP6) and scenario (SSP 245, SSP 585, RCP 4.5, RCP 8.5). For all boxplots the change is computed from the historical simulation for 1985-2014 to the select scenario for 2070-2099.

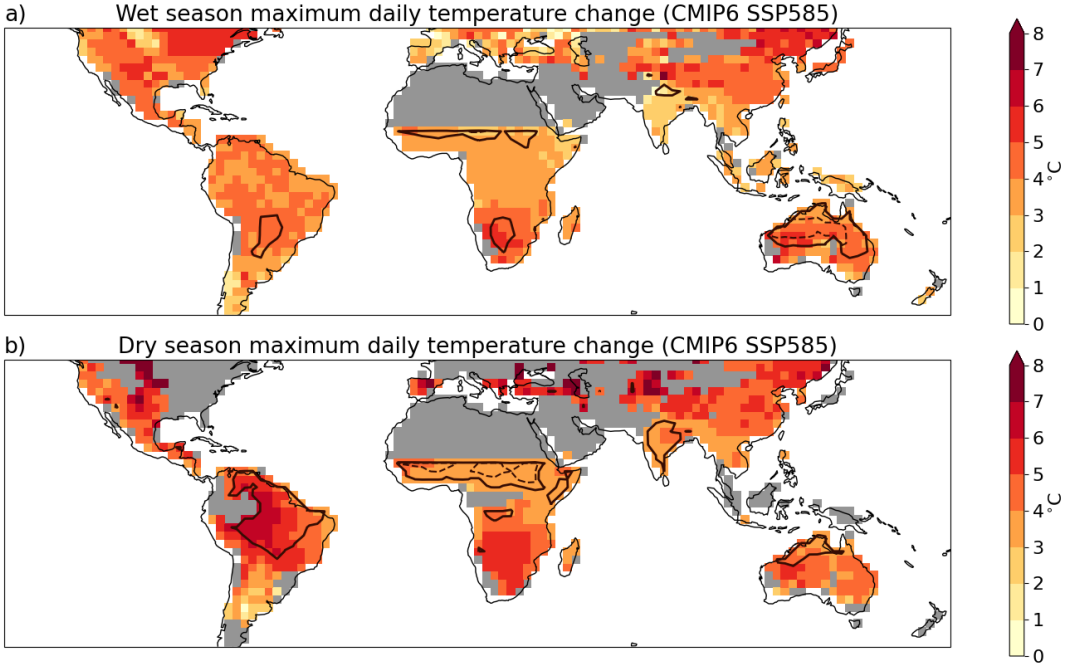

FIG. 11. CMIP6 multi-model median change in a) mean wet season maximum daily temperature and b) mean dry season maximum daily temperature for the SSP585 scenario over 2070-2099 compared with the historical simulation over 1985-2014. The contours indicate where the CMIP6 multi-model median wet and dry season mean daily maximum temperature is greater than 35°C for the historical simulation over 1985-2014 (dashed line) and the SSP585 simulation over 2070-2099 (solid line). In all panels grey regions indicate where at least 50% of the models do not give a value (dry year round or wet year round in the dry season plots).

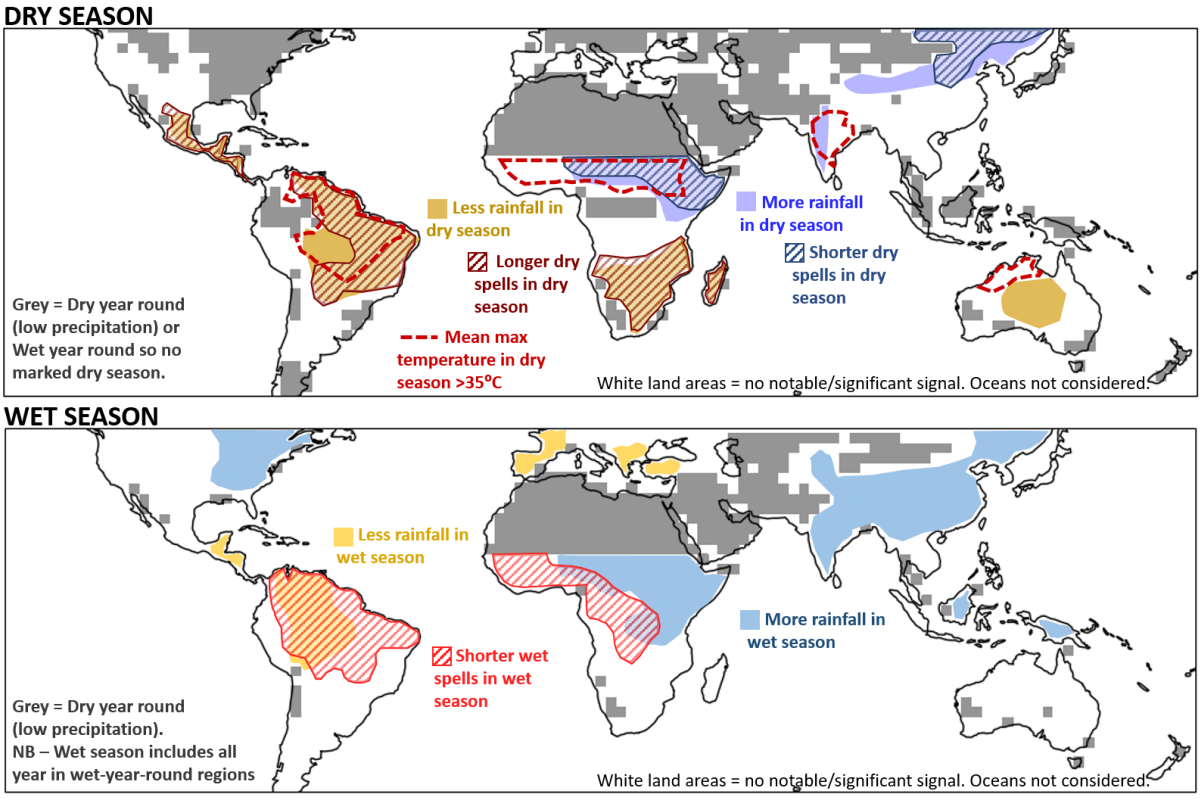

FIG. 12. Schematic summarising the changes in wet/dry season rainfall and wet/dry spell lengths in wet/dry seasons found here; the top panel is for dry seasons and the bottom row is for wet seasons (including regions that are wet year round).

(Top) Longer dry spells and lower rainfall during the dry season are found over Central and South America and Southern Africa. Shorter dry spells and more rainfall during the dry season are found over East Africa and parts of Asia and the Sahel.

(Bottom) More rainfall in the wet season is found over East Africa and Asia. Less rainfall in the wet season is found over northern South America. Reductions in the length of wet spells in the wet season are found over South America and West and Central Africa.